The United Nations University

GEOTHERMAL TRAINING PROGRAMME
Orkustofnun, Grensásvegur 9,
IS-108 Reykjavík, Iceland

Reports 2003
Number 3

RESERVOIR ASSESSMENT OF ZUNIL I & II GEOTHERMAL FIELDS, GUATEMALA

Francisco Asturias
Instituto Nacional de Electrificación - INDE
Unidad de Desarrollo Geotérmico - UDG
7a Av. 2-29 Zona 9, C.P. 01009, Guatemala City
GUATEMALA
fasturias@inde.gob.gt

ABSTRACT

Conceptual models for Zunil I and II are presented from careful analysis of reservoir temperatures and initial pressures. The Zunil I reservoir is divided into an upper and lower reservoir by a lithological contact between the granitic formation and overlying volcanic rocks. Wells producing from the upper reservoir yield less total output than wells that produce from the deeper reservoir. There appears to be a main upflow in the western part of Zunil I at the intersection of northeast and northwest regional fault trends. A second upflow may be present near the eastern edge of Zunil I, possibly connected as a line source along a northeast trending fault to the main upflow in the western area. Pressure potentials are highest in the west, suggesting fluid upflow, with outflows to the northeast and east. The Zunil II area shows higher overall temperatures at shallower depths than Zunil I with a source upflow possibly located in the southeast area. Temperature and pressure distributions suggest that fluids flow to the northwest from the upflow zone. Wellbore simulations of shallow and deep producing wells show that cooling of fluids from re-injection of brine will not have an adverse effect on total steam output but will maintain pressures in the reservoir. A volumetric assessment of the Zunil II reserve shows that there is potential for 35 MWe for the next 25 years.

1. INTRODUCTION

The Zunil geothermal area is located 220 km west of Guatemala City (Figure 1). The Zunil geothermal area is divided into Zunil I and Zunil II fields. Exploration of Zunil began as early as 1970 by INDE, the national utility company. In 1981, it was decided to make a national inventory of all geothermal resources of Guatemala to understand and define the most promising areas for exploitation. Pre-feasibility studies were carried out with funds from INDE and a donation from the Latin American Energy Organization (OLADE and BRGM, 1982). The study classified seven areas; of them Zunil I and II were found to be among the most promising and were given priority. Zunil I has been under exploitation since 1999, when Ormat Inc. commissioned a binary geothermal power plant with an installed capacity of 24 MWe.

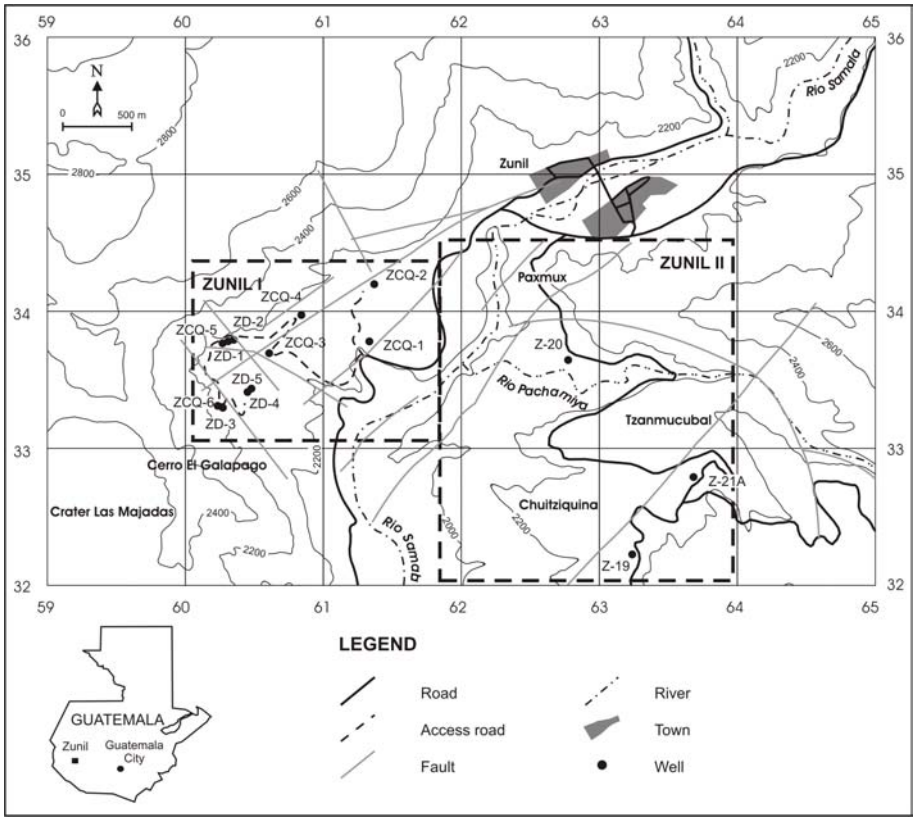

FIGURE 1: Overview of the Zunil geothermal area showing location of wells and major geologic structures

During 1980 and 1981, INDE drilled 6 production wells in Zunil I to determine the geothermal potential of the Zunil I reservoir. The deepest of these wells, ZCQ-6 was drilled to 1142 m depth. It was estimated that Zunil I could produce enough steam to sustain 24 MWe production for 25 years (Palma-A. and Garcia, 1995). The drilling confirmed the existence of a single-phase liquid (270-290°C) reservoir below 1000 m depth. Additional wells were needed to increase total production. From 1991-2000, INDE drilled 5 new wells, targeting the deep reservoir. The deepest well, ZD-3 was drilled to 2370 m. Of the 11 production wells drilled in Zunil I, 5 wells are used for production and 2 for re-injection. Table 1 shows the general characteristics of wells drilled in the Zunil area.

TABLE 1: General characteristics of wells in Zunil I and II

Well No.	Depth (m)	Elevation (m a.s.l.)	Eastings	Northings	Depth to casing shoe and size (m ")	Remarks
ZCQ-1	1310	2004	61.355	33.792	765 $9\,^{5}/_{8}$	Reinjector
ZCQ-2	812	2059	61.381	34.201	516 $9\,^{5}/_{8}$	Reinjector
ZCQ-3	1041	2077	60.619	33.686	590 $9\,^{5}/_{8}$	Producer
ZCQ-4	1025	2117	60.891	34.013	447 $9\,^{5}/_{8}$	Producer
ZCQ-5	1080	2175	60.260	33.780	751 $9\,^{5}/_{8}$	Offline
ZCQ-6	1142	2175	60.240	33.300	600 $9\,^{5}/_{8}$	Offline
ZD-1	1516	2175	60.302	33.837	648 $9\,^{5}/_{8}$	Producer
ZD-2	1784	2175	60.340	33.828	747 $9\,^{5}/_{8}$	Producer
ZD-3	2370	2175	60.250	33.250	1122 $9\,^{5}/_{8}$	Offline
ZD-4	1226	2120	60.448	33.406	942 $9\,^{5}/_{8}$	Producer
ZD-5	1776	2120	60.460	33.420	1043 $9\,^{5}/_{8}$	Observation
Z-19	576	2360	63.680	32.650	403 NQ*	Observation
Z-20	364	2140	62.900	33.650	347 NQ*	Observation
Z-21A	757	2336	63.300	32.300	296 $9\,^{5}/_{8}$	Observation

NQ*: 70 mm

Zunil II is located east of Zunil I across Rio Samala (See Figure 1). From 1989 to 1992, INDE carried out extensive geoscientific studies in Zunil II. Two slim holes and one production well were drilled. The deepest well, Z-21A reached a depth of 757 m and a maximum temperature of 244°C was encountered. Although drilling did not penetrate into the main reservoir, it confirmed the existence of a deep reservoir residing below a steam zone (West Japan Engineering Consultants et al., 1995). Zunil II has an estimated potential of 50 MWe for 25 years of utilization (West Japan Engineering Consultants et al., 1991).

At present, INDE plans to explore the Zunil II geothermal field in order to evaluate the reservoir potential. One re-injection and two production wells will be drilled this year (2003). Directional wells will be drilled towards the northwest area of Zunil II beneath Rio Samala and in the nearby Paxmux area to confirm the existence of a deep reservoir and upflow zone. Evaluation of the reservoir will be done by installing a 5 MWe backpressure geothermal turbine at the beginning of 2005 and operate it one year (Palma-A. and Manzo, 2000). Future planning and construction of a 24 MWe plant will depend on the results of the reservoir evaluation.

This report presents a reservoir assessment study for the Zunil I and Zunil II geothermal fields. A revised conceptual model is presented that includes both Zunil I and II. A connection between the reservoirs will aid in defining a strategy for exploitation of Zunil II and suggest how production will affect reservoir conditions in Zunil I. A detailed evaluation of initial reservoir temperatures and pressures was done. Detailed cross- and planar-sections are presented that reflect initial conditions. Finally, a volumetric assessment based on temperature distributions of the Zunil II geothermal field was carried out using Monte-Carlo simulation in order to estimate the reserve potential.

2. HISTORY OF EXPLORATION

2.1 Regional tectonics

Guatemala is located in the northern part of Central America. Tectonic activity is controlled by the relative motion of converging plates. To the south, oblique subduction of the Cocos plate has given rise to intense volcanic activity. A volcanic chain extends from east to west and rises sharply from the coastal low lands in the south. The volcanic activity is characterized by explosive volcanic eruptions and caldera complexes. Shear left lateral faulting in central Guatemala has created segmentation and extension along the volcanic belt (Stoiber and Carr, 1974). This occurs in response to the northeastern migration of the trailing edge of the Caribbean plate (Figure 2). Thinning of the crust eases the migration path of buoyant magma bodies as they make their way to the surface. Regional faulting, combined with intrusive bodies as a local heat source, creates ideal conditions for geothermal activity.

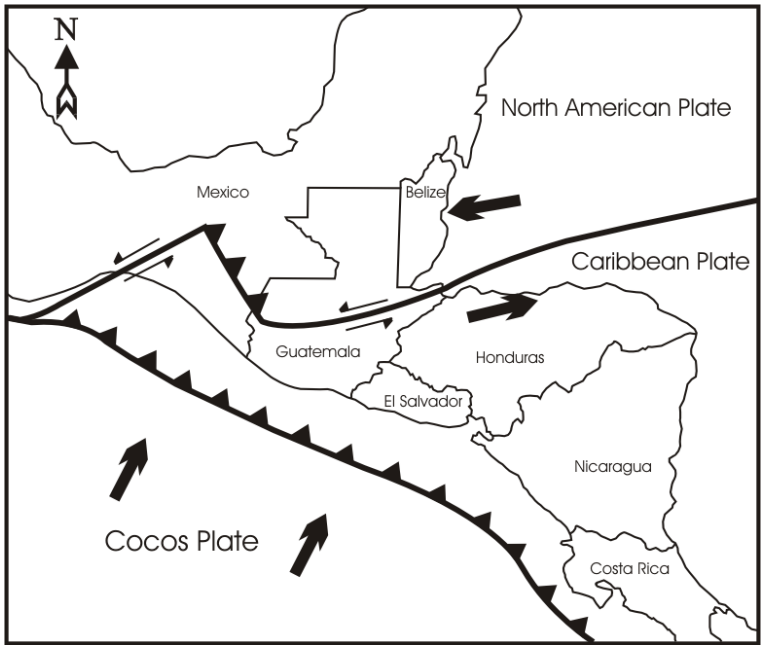

FIGURE 2: Tectonic map of northern Central America showing relative motion of plates (modified from Weyl, 1980)

2.2 Geology

The structural settings for the Zunil geothermal area are marked by the intersection of two regional trends. The northeast trending Zunil fracture zone intersects the lower structural margins of the Queztatenango Caldera (Figure 3). On a local scale, a smaller northwest trending fault system has also been mapped. Evidence for the Quetzaltenango caldera include the occurrence of large circular features visible on satellite photos, thick sequences of ash flow tuffs with no known source areas, and the occurrence of ash flow tuffs near the base of the volcanic sequence in production wells (Foley et al., 1990). A smaller scaled semicircular structure bounds the east and south margins of Zunil II. This depressed structure defines a smaller collapsed caldera, 4 km in diameter from Volcan de Zunil. Northeast and northwest trending faults control the movement of fluids and are reflected in topography and in gravity data.

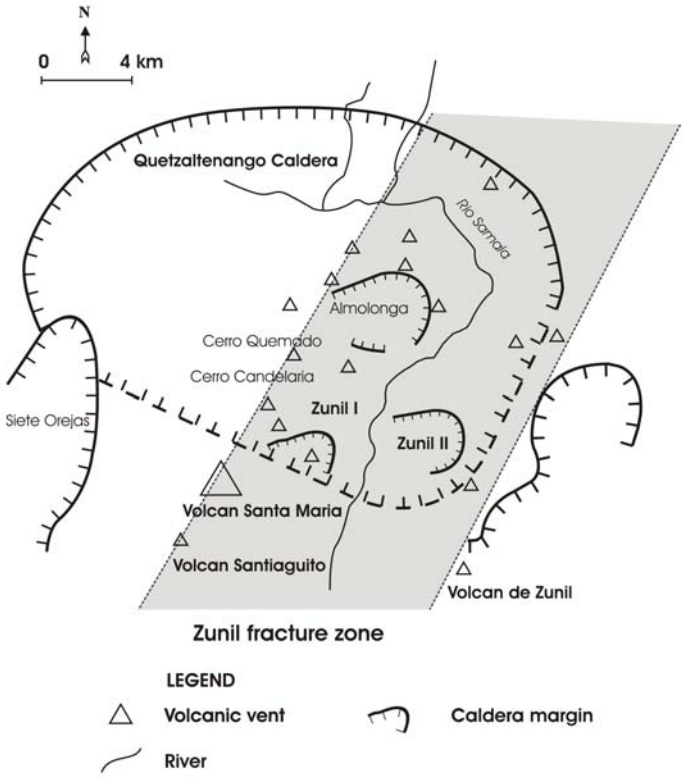

FIGURE 3: Map of Zunil area showing major volcanic features; the Zunil fracture zone is shown as a shaded area (modified from Foley et al., 1990)

Lithology from production wells show that a deep granitic formation is overlain unconformably by thick deposits of lava flows and ash-flow tuffs of andesitic to dacitic composition (ELC-Electroconsult, 1980). These sections are overlain by thin deposits of alluvium, landslides, and pumaceous deposits. The base of the volcanic section in wells ZCQ-3, 5 and 6 encountered intense veining and brecchiation and losses of circulation. This contact represents a permeable zone associated with faulting. In Zunil I, the granitic formation is found at a depth of 1092 m a.s.l. in well ZCQ-4, and shallows out towards the west to 1324 m a.s.l. in well ZCQ-1. Deeper drilling of ZD wells indicated faulting that extends into the granitic formation where a deeper reservoir resides. In Zunil II, the basement was encountered at a shallower depth of 1951 m a.s.l. in well Z-21A.

2.3 Hydrothermal alterations

In Zunil I, hydrothermal alteration within production wells increases downward and can be divided into an upper argillic zone and a lower propylitic zone. Mineral assemblages in hydrothermal veins suggest that geothermal fluids migrate upward in the granodiorite through permeable fault zones and upward through the overlying volcanics where boiling occurred in response to cooling (Córdon y Mérida et al., 1990). A steam-heated cap has developed over the geothermal system, created by condensation of steam and CO_2 gases, and mixing of colder groundwater. The occurrence of illite veining created in rocks containing quartz + epidote + calcite veins suggest that secondary alterations are well developed and are migrating downwards into the deeper reservoir. Distribution of secondary fluid alteration suggests that the steam-heated cap increases in thickness to the west and that an upflow zone is in the vicinity of wells ZCQ-3, 5, and 6 (Moore et al., 1990).

2.4 Geophysics

Resistivity and gravity surveys are strongly affected by hydrothermal alteration variations. Resistivity soundings reveal hydrothermal alterations at relatively shallow levels in Zunil I. A shallow, low-resistivity layer overlays a high-resistivity core that may indicate change in alteration from clay minerals towards chlorite-epidote within the volcanic rocks. The conductive layer thickens from west to east and south, and is consistent with an upflow zone near well ZCQ-6 (Figure 1). The thickness of the high-resistivity basement is not well defined due to effects of topographic variations and inhomogeneities within the volcanic rocks. Gravity surveys show several highs within the field that represent higher density values in the shallow volcanic rocks due to hydrothermal alterations (Foley et al., 1990).

Resistivity soundings show a greater degree of details in Zunil II. Two separate resistivity anomalies were identified, one around the intersection of Rio Samala and Rio Pachamiya, and another in the Chuitziquina area. The base of the low-resistivity zone is consistent with depths to the granitic formation with higher alteration into that formation. Gravity surveys are also consistent with the depth to the granitic formation. The surveys also pointed out an east-northeast trending horst structure between Zunil I and II beneath Rio Samala bounded to the west by a graben structure. The graben deepens to the southwest and is bounded by another horst structure trending east-northeast centred at Chuitziquina. This is in agreement with the resistivity anomaly in the same area. The horst separates Zunil II into a northern section around Rio Samala, and a southern zone south of Chuitziquina.

2.5 Geochemistry

Water samples from deep wells and springs define two distinct fluid compositions derived from different sources. In Zunil I, fluids are coming from a shallow steam heated reservoir underlain by a deeper reservoir. The shallow reservoir results from mixing of meteoric waters and steam condensate created as migrating steam cools at shallow depths. Fluid produced from ZCQ wells are a mixture of two fluid types both with a greater degree of dilution in the east. Wells ZCQ-3 and 6 show the least amount of dilution, consistent with an upflow zone in the area (Adams et al., 1990). Water samples from wells drilled in Zunil II have shown that also there a shallow steam cap overlays a deeper reservoir as in Zunil I. Low contents of non-condensable gases indicate the existence of a deeper liquid reservoir.

Geothermometry of hot springs from Zunil I and II give estimated temperatures of 290°C and 250-280°C, respectively, for the reservoir fluids. Isotope analyses from Zunil I and II show that fluids from the deeper reservoirs have similar isotopic compositions as waters from Rio Samala that drain the Quetzaltenango Valley and Cantel areas to the north and northwest. Recharge waters originate in the north and northeast and migrate towards the Zunil systems. The recharge feeds Zunil I from the north and east, while Zunil II is recharged from the north. In both fields, local meteoric water flows downward and recharges a shallow reservoir of mixed composition. The two underground flows seem to be mixing at shallow depths around the intersection of Rio Samala and Rio Pachamiya (Lima and Palma-A., 2000). Fluid chemistry variations from deep wells suggest non-homogenous reservoir conditions for Zunil I. No deep connection has yet been found between Zunil I and II, although both reservoirs share similar chemical composition. Fluid age estimates from hydrogen isotopes show that the fluid is of old water (Adams et al., 1990).

3. DOWNHOLE TEMPERATURE AND PRESSURE

Downhole data, or logging, is a valuable tool to gain information on the physical conditions of the reservoir and well performance. It provides a picture, although indirectly, of the local thermodynamic and chemical conditions in the reservoir. However, caution must be used when interpreting logs as measurements are not made directly in the reservoir but in the well where internal flows and boiling can

cause disturbances and give misleading results even though the well is shut-in. (Stefánsson and Steingrímsson, 1990).

3.1 Collection of data

Temperature and pressure logs from Zunil wells were collected from various integrated test reports. The logs were taken during drilling, warm-up, flowing and shut-in periods. A total of 200 temperature and 83 pressure logs were collected. Many had to be digitized from paper, and saved as computer text files. The data was saved into a PC computer and downloaded to an Oracle database. Reservoir temperatures and pressures for each well were estimated and downloaded as well. Tables 2 and 3 show the estimated reservoir temperatures and initial pressures for each well in Zunil I and II. Storing all the data on an Oracle database was helpful when generating graphs of each well and creating cross- sections and planar-sections of the study areas. Each well was given an ID number and each log was given a tracking number. The compiled data is presented on single graphs for each well. This gave a clearer picture of the downhole conditions for each well and finally resulted in estimated natural state conditions of the reservoir in the Zunil I and II geothermal fields. Reservoir temperatures and initial pressures for each well are described in Appendix I.

3.2 Zunil I wells

Reservoir temperatures and initial pressures for wells in Zunil I are shown in Figures 4 and 5. Temperatures in the lower reservoir are close to 300°C. The upper and lower reservoir boundary is at 1100 m a.s.l. The upper reservoir has temperatures at saturation. Initial pressures vary a great deal in Zunil I. This suggests heterogeneity in the upper reservoir. The highest reservoir pressures are measured in wells ZD-1 and 2. Lower pressures are seen in wells that produce from the shallow reservoir. A high-pressure drawdown restricts the flow of fluids into the wells. The deeper wells show less pressure drawdown at the feedzones and more fluid is able to enter the well.

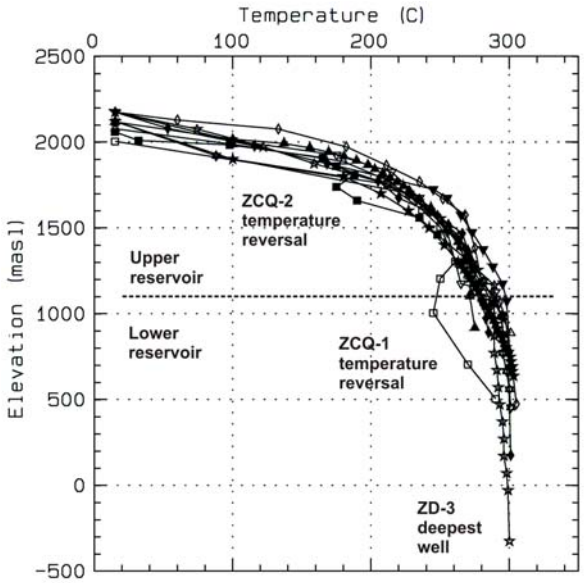

FIGURE 4: Estimated reservoir temperatures for Zunil I wells

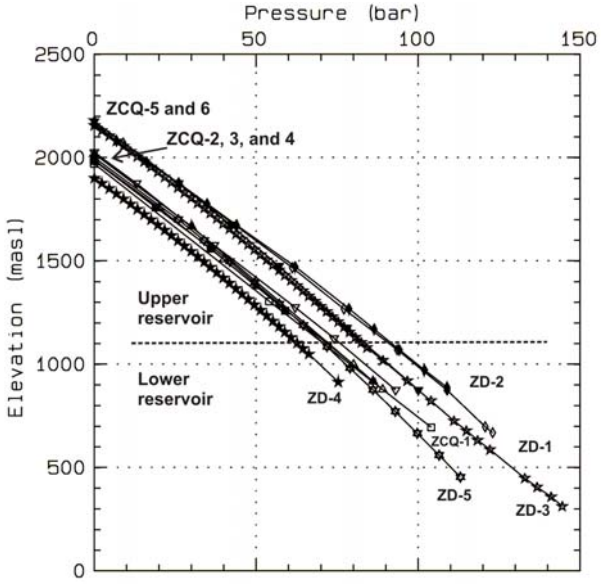

FIGURE 5: Estimated initial pressures for Zunil I wells

TABLE 2: Estimated reservoir temperatures for wells in Zunil I and II geothermal fields

Depth (m)	ZCQ-1	ZCQ-2	ZCQ-3	ZCQ-4	ZCQ-5	ZCQ-6	ZD-1	ZD-2	ZD-3	ZD-4	ZD-5	Z-19	Z-20	Z-21A
0	15	15	15	15	15	15	15	15	15	15	15	15	15	15
100	94	120	108	100	67	67	134	56	74	72	52	48	66	43
200	173	175	185	180	131	119	182	118	121	129	88	81	145	72
300	220	179	215	208	195	172	208	168	165	173	152	152	193	107
400	237	190	230	228	222	224	234	196	204	203	215	196	216	182
500	250	235	245	243	235	255	242	213	230	224	240	210	233	209
600	256	248	253	255	245	262	263	247	247	239	252	222	247	229
700	261	263	260	263	255	269	268	263	260	252	262	235		243
800	250	274	265	268	258	276	272	270	269	262	271			255
900	248	281	269	271	262	283	276	274	277	270	279			265
1000	245	288	269	272	265	290	279	276	288	278	286			274
1100	253		271	273	291	292	290	278	293	285	292			
1200	262		273	274	293	294	295	281	289	291	295			
1300	270					297	296	287	289	296	295			
1400	280					299	297	296	289		296			
1500	290					301	300	297	291		299			
1600							300	298	292		300			
1700								299	293					
1800								300	295					
1900								301	296					
2000								302	296					
2100									298					
2200									299					
2300									299					
2400									300					
2500									300					

TABLE 3: Initial reservoir pressures for the wells in Zunil I and II geothermal fields

Depth (m)	ZCQ-1	ZCQ-2	ZCQ-3	ZCQ-4	ZCQ-5	ZCQ-6	ZD-1	ZD-2	ZD-3	ZD-4	ZD-5	Z-19	Z-20	Z-21A
100	5	2	1	0	4	0	0	7	7	7	7	4	3	0
200	13	11	10	9	13	9	8	16	16	16	16	13	12	9
300	22	19	18	17	21	17	17	26	24	24	24	21	20	18
400	30	28	26	26	29	26	26	35	32	32	32		29	26
500	38	36	34	34	37	34	35	44	40	40	40		37	34
600	46	44	42	42	45	42	43	53	48	47	48			
700	54	51	50	50	54	50	52	62	55	54	55			
800	62	59	58	58	62	57	60	70	63	61	62			
900	70		66	67	70	64	68	78	70	68	69			
1000	79		74	74	78	71	76	86	77	75	76			
1100	87		82		85	78	85	94	85		83			
1200	95		89		93	85	93	102	92		90			
1300	103				93		101	110	100		96			
1400							109	118	107		103			
1500							116	126	115		109			
1600								134	123		122			
1700								143	131					
1800								151	139					
1900								159						
2000								167						

3.3 Zunil II wells

Reservoir temperatures and initial pressures for wells in Zunil II are shown in Figures 6 and 7. Temperatures measured in the wells are close to saturation. A conductive cap layer overlays a convective system at saturation conditions. Temperatures increase and may reach 300°C in the granitic formation where a liquid reservoir may reside. This can only be confirmed by drilling deeper into Zunil II. Depressed water levels in the wells from accumulated steam and gas may be the reason for the differences in the estimated boiling point with depth (BPD) profiles. Initial pressures were estimated to be hydrostatic down to the bottom of the wells.

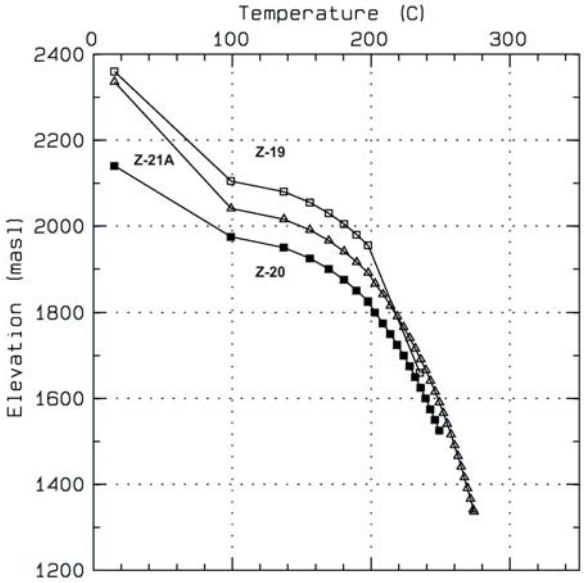

FIGURE 6: Estimated reservoir temperatures for Zunil II wells

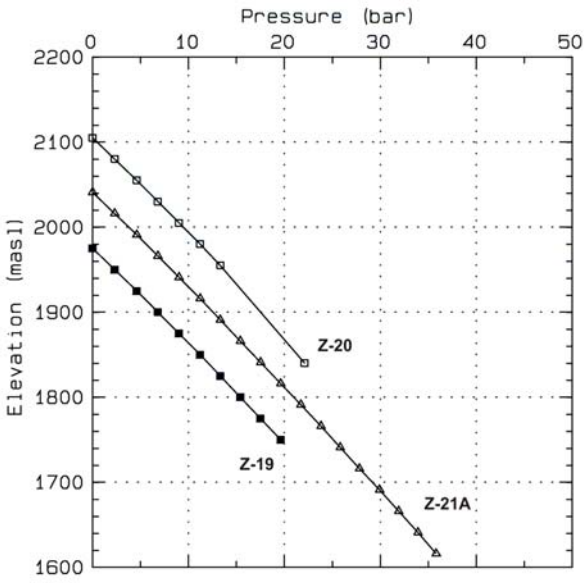

FIGURE 7: Estimated initial pressures for Zunil II wells

4. DISCHARGE AND INTERFERENCE TESTS

Carrying out interference tests when a well is discharged can give valuable information on significant sections of reservoir behaviour and defining its hydrological properties over an extensive distance. By removing fluid from a discharging well, pressure drawdown with respect to time can be measured in nearby wells. The resulting drawdown curve is compared to a line source solution for a reservoir that is horizontal and uniform in thickness, homogenous, with constant porosity and permeability, or the so called Theis model. If the results match, the hydrological parameters, transmissivity and storativity can be calculated. Interference tests can give other useful information on reservoir properties such as boundary conditions and relative permeability between wells (Grant et al., 1982).

In high-temperature reservoirs, both steam and water may be present. The compressability of steam is much greater than water and can give much higher values for transmissivity and reservoir storativity. This should be taken into consideration when interpreting reservoir properties near the wellbore.

4.1 Discharge tests

Table 4 shows the measured parameters during flow tests of wells in Zunil I. Concurrent downhole pressure changes were monitored in nearby wells to get information on the hydraulic condition of the reservoir. Pressure was monitored using capillary tubing and downhole chambers as discharging wells were flowed to a silencer. A simultaneous injection test in well ZCQ-2 was carried out using discharged

waters from well ZCQ-3. It is important to note that there is a one-month delay in pressure response in well ZCQ-1 after shut-in of production wells ZCQ-3 and 4 that may reflect reservoir changes that are not representative of the reservoir. Several wells were affected by inaccurate measurements from high wellhead pressures that suppressed the water level below the chamber.

TABLE 4: Well characteristics during discharge tests. ZCQ wells were tested in 1989 and ZD wells were tested in 1992-93 (Córdon y Mérida et al., 1993) (water and steam flow are calculated using a separator pressure of 11 bar)

Well No.	WHP (bar)	Enthalpy (kJ/kg)	Qt (kg/s)	Qw (kg/s)	Qs (kg/s)
ZCQ-3*	7, 9	1492, 1302	22.2, 33.3	14.3, 24.6	7.9, 8.7
ZCQ-4	7	2520	13.9	1.8	12.1
ZCQ-5	10	2436	9.2	1.6	7.6
ZCQ-6	8	1512	13.9	8.8	5.1
ZD-1**	10, 12	1492, 1344	83.3, 91.7	53.7, 65.9	29.6, 25.8
ZD-2**	10, 13	1512, 1492	54.2, 66.7	44.2, 42.7	20.0, 24.0
ZD-3	6	1554	22.2	13.6	8.6
ZD-4	11	1470	25.5	14.4	11.1

* Data values from short-term test and long-term test, respectively.

** Data values from single well discharge and combined well discharge of ZD-1 and 2.

The first tests for ZCQ wells were carried out from March 20th to October 28th, 1989. A second set of tests were carried out from February 24th to March 9th, 1992 when wells ZD-1, 2, and 3 were production tested. Each well was discharged separately, as well as a combined discharge of all three wells.

4.2 Interference tests

The results indicate that the wells had high initial decline rates and additional wells will be needed to maintain production in Zunil I (Menzies et al., 1990). Calculated values for transmissivity and storativity for wells that responded to discharging wells are shown in Table 5.

TABLE 5: Interference test results from Zunil I conducted in 1989 and 1992 (Córdon y Mérida et al., 1993)

Observation well	Production well	Distance (m)	Transmissivity (Dm)	Storativity (m/bar)	Remarks
ZCQ-1	ZCQ-3	725	8.50	0.01	
ZCQ-4	ZCQ-3	300	1.60	0.024	
ZCQ-3	ZCQ-3	-	5.18	0.024	Buildup
ZCQ-3	ZD-1	250	61.0	0.480	
ZCQ-3	ZD-1/2	250	70.0	0.200	
ZCQ-4	ZD-1	600	70.0	0.500	
ZCQ-5	ZD-1	50	30.5	0.017	
ZCQ-5	ZD-1/2	50	15.0	0.005	
ZCQ-6	ZD-1	500	27.5	0.042	
ZCQ-6	ZD-1/2/3	-	30.0	0.010	
ZD-1	ZD-2/3	-	40.0	0.005	
ZD-2	ZD-1	50	11.0	0.042	
ZD-2	ZD-3	500	10.0	0.020	
ZD-3	ZD-1/2	500	50.0	0.001	

The transmissivity for wells ZD-1 and 2 are an order of magnitude higher than wells producing from the shallow reservoir. It is clear that wells ZD-1 and 2 are the most productive wells in the field. These wells have higher permeability than all other wells in Zunil I. This may be due to the nature of the reservoir that resides in the fractured granitic formation at depth. There appears to be less pressure drawdown from the reservoir to the feedzones which yields higher flow rates and prevents flashing in formation.

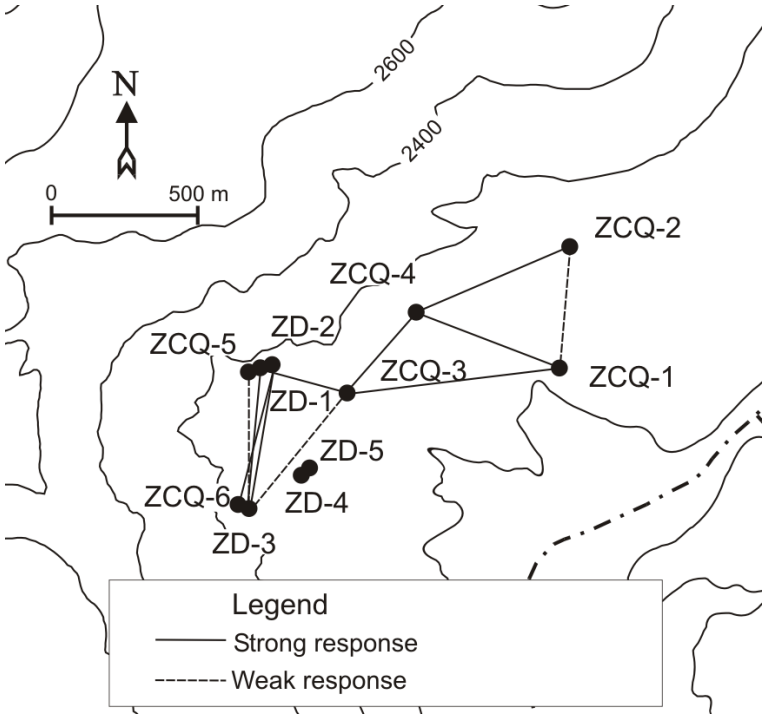

FIGURE 8: Interactions between wells from interference data (modified from Córdon y Mérida et al., 1991)

The interaction between wells from the interference tests are shown in Figure 8. Analysis of interference data shows that some wells had a very good connection while other wells did not respond to discharge or injection at all. There is a strong connection for the central wells ZCQ-3, 4, and 1. There is no visible defined connection between the central wells and well ZCQ-2. There seems to be little connection between the western area of Zunil I and the central wells. In particular, well ZCQ-6 did not respond to production or injection from wells in the central field and seems to be isolated completely. The wells located in the western area show a strong connection between them. This is consistent with the pattern of faulting and may indicate that some faults are acting as hydraulic barriers while others as conduits.

5. WELLBORE SIMULATIONS

The simulator HOLA was used to simulate the wellbore conditions that influence the transport of fluid from the reservoir to the surface. The simulator numerically solves a set of differential equations that describe the steady-state energy, mass and momentum flow in a vertical pipe for single or two-phase flow. The governing equations are the following (Björnsson et al., 1993):

$$\frac{dm}{dz} = 0 \tag{1}$$

$$\frac{dP}{dz} - \left[\left(\frac{dP}{dz} \right)_{fri} + \left(\frac{dP}{dz} \right)_{acc} + \left(\frac{dP}{dz} \right)_{pot} \right] = 0 \tag{2}$$

$$\frac{dE}{dz} \pm Q = 0 \tag{3}$$

where m = Total mass flow (kg/s);
P = Pressure (Pa);
E = Total energy flux in the well (J/s);
z = Depth coordinate (m);
Q = Ambient heat loss over a unit distance (W/m).

The governing equation for flow between the well and the reservoir is:

$$m_{feed} = PI\left[\frac{k_{rl}\rho_l}{\mu_l} + \frac{k_{rg}\rho_g}{\mu_g}\right]\left(P_r - P_w\right) \quad (4)$$

where m_{feed} = Feedzone flowrate (kg/s);
PI = Productivity index (m^3);
k_r = Relative permeability of the phases (subscript *l* for liquid and *g* for steam);
μ = Dynamic viscosity (subscript *l* for liquid and *g* for steam) (kg/ms);
ρ = Density (subscript *l* for liquid and *g* for steam) (kg/m^3);
P_r = Reservoir pressure (Pa);
P_w = Pressure in the well (Pa).

Values of enthalpy, wellhead pressure, feedzone depth and pressure, measured reservoir pressure, and geometry of the well are entered into the wellbore simulator. By performing a series of iterations, a feedzone productivity index is defined that matches the measured results. Once a value for the productivity index has been derived, predictions can be made. Modelling the specific behaviour of the reservoir is done by varying values of the physical properties of the reservoir and the fluid. The characteristics of the well are be shown as calculated output curves of total flow versus wellhead pressure. A flowing profile will also be generated that can be compared to a measured profile.

Measured data during discharge of wells ZD-1, ZCQ-3 and 6 (see Table 4) were analyzed in order to find out the behaviour of the wells and the nearby reservoir. Figure 9 shows the output curve of ZD-1, a deep producing well. Output curves of shallow producing wells ZCQ-3 and 6 are shown in Figures 10 and 11, respectively. Definition of the wellbore geometry for each well is done down to the feedzone depth. Measured static and flowing logs have also been plotted to compare the calculated pressure conditions during flow.

Well ZD-1 was simulated using a productivity index of 0.36×10^{-11} m^3 and by matching several outputs with corresponding wellhead pressures. The matched output curve shown represents the initial conditions when the well was first flowed (Figure 9). Production in the well has since dropped from 90 to 55 kg/s.

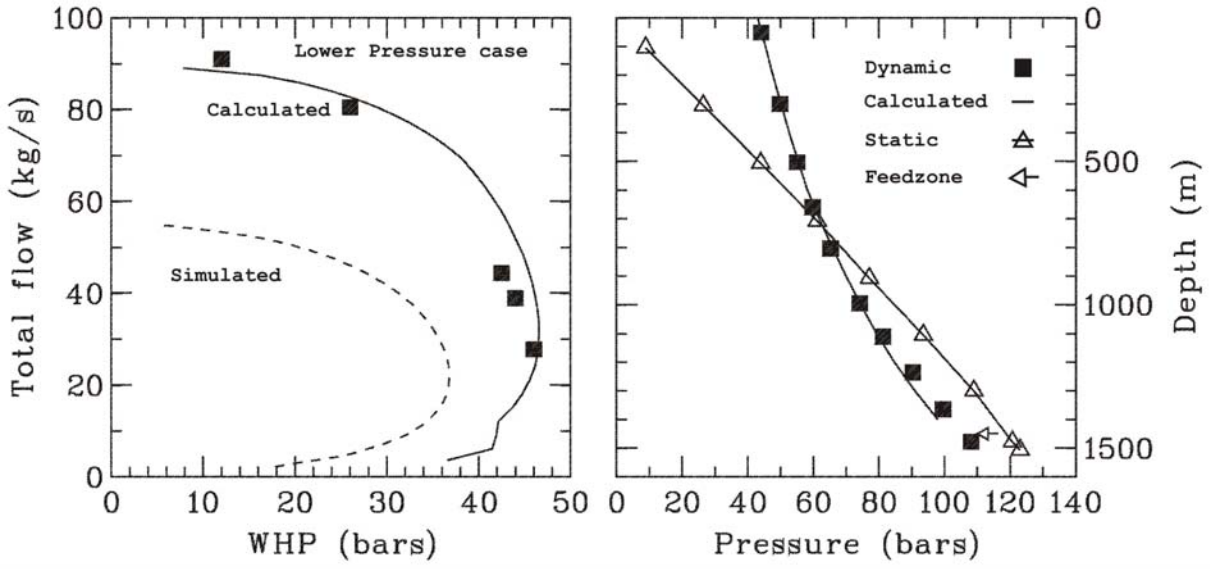

FIGURE 9: Measured output curves for well ZD-1 and logs showing pressure for static and flowing conditions; the calculated output curve represents initial condition whereas the simulation curve corresponds to flow when substantial pressure drawdown has developed

The drop in production was best simulated by lowering the pressure in the reservoir at the feedzone by 30 bar with a 10 bar wellhead separator pressure as reference. This is assumed to be the pressure drop in the reservoir since the well came online. As shown by the simulated output, the well matches the field output of the well. It can be shown that the well has experienced a substantial pressure drop in the surrounding reservoir.

Well ZCQ-3 was modelled using a productivity index value of 0.28 $\times 10^{-11}$ m^3 matching the measured values of enthalpy and flow. Pressure in the reservoir was then lowered by 10 bar (Figure 10). The calculated output curve shows a decrease in total output for the well. The output decreases from 22 to 14 kg/s for a wellhead separator pressure of 10 bar used in Zunil I.

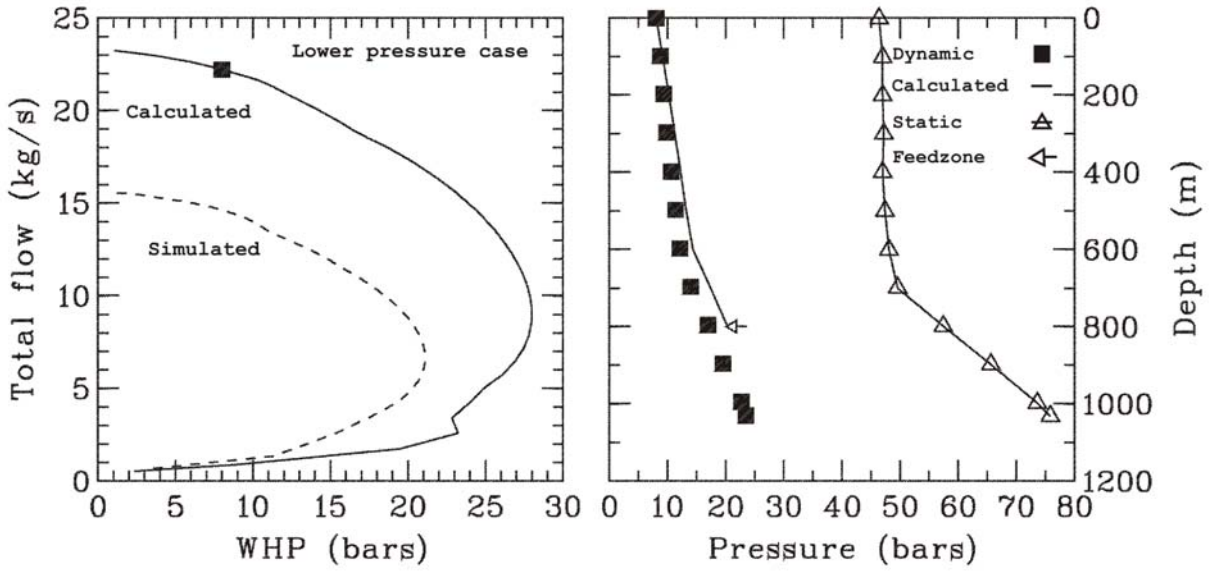

FIGURE 10: Measured output curves for well ZCQ-3 and logs showing pressure for static and flowing conditions; output curves correspond to little or large pressure drawdown

On the other hand, well ZCQ-6 was modelled with a feedzone productivity index of 0.08 $\times 10^{-11}$ m^3. The well was made to show a decrease in fluid enthalpy from the value of 1512 to 1200 kJ/kg. The resulting output curve showed an increase in production. At the same wellhead separator pressure of 10 bar, the total flow of the well is raised by 8 kg/s (Figure 11).

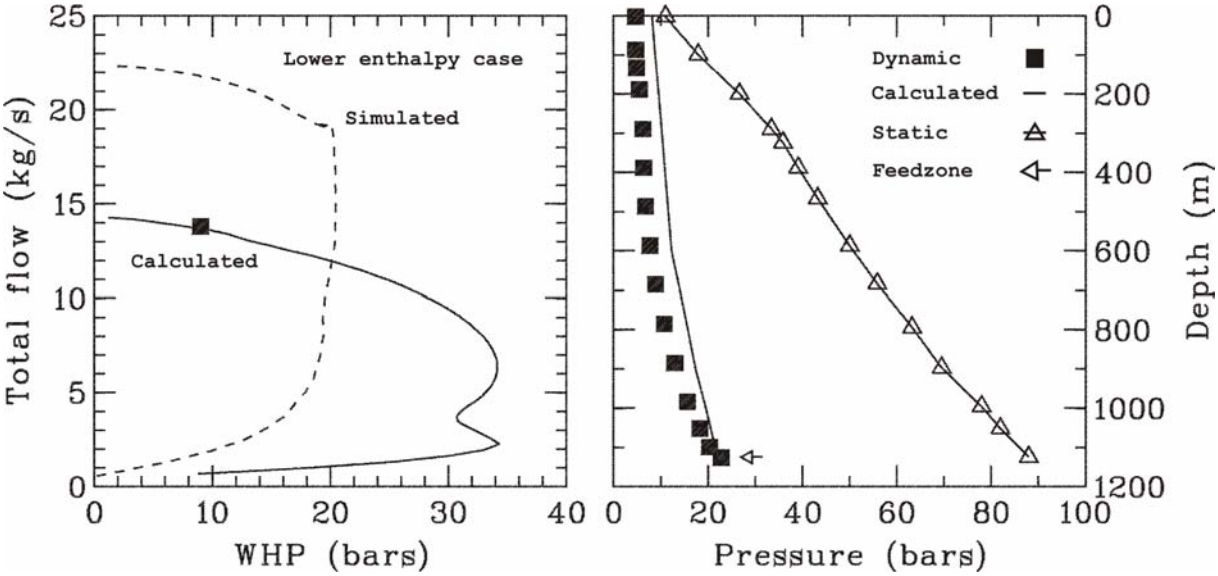

FIGURE 11: Calculated output curves for well ZCQ-6, different well enthalpies and logs showing pressure for static and flowing conditions

The calculated changes in output by lowering the enthalpy tells something about the fluid in the reservoir and the effects of re-injection. A drop in enthalpy can be an indication that temperatures in the reservoir are decreasing. This can happen mainly when there is an increase of colder recharge waters in response to a pressure drop in the reservoir. Another reason for lower reservoir temperatures can be the result of thermal breakthrough from re-injected waters. This phenomenon of cooling due to re-injection has been observed in Ahuachapán, Palinpinon, and Svartsengi (Stefánsson, 1997). As described above, a decrease in enthalpy was followed by an increase in total flow for well ZCQ-6. This happens because the mobility of water is greater when the relative fraction of the steam phase in the two-phase mixture decreases relative to the water component. The well produces more water, and since density of water is greater than steam, more mass will flow from the well. Surprisingly, although more total mass is produced, the well will not produce more total steam. It is also important to note that total steam production does not decrease significantly either. The total steam produced from well ZCQ-6 stays relatively constant as the enthalpy of the fluid decreases.

This is very favourable in Zunil I, where all produced mass is injected back to maintain pressure in the reservoir. Fear of thermal breakthrough has frequently been the deciding factor against using re-injection in geothermal operations (Stefánsson, 1997). This model demonstrates that thermal breakthrough from re-injection or recharge from cooler fluid will not have adverse effects on steam production and will only increase the amount of water that is produced for the shallow producing wells that flash in formation. If re-injection is not utilized to maintain pressure levels, the pressure will decline. The simulated parameters for well ZD-1 and ZCQ-3 show that this will result in a drop in total mass flow.

6. REVISED CONCEPTUAL MODEL FOR ZUNIL I AND II RESERVOIRS

A conceptual reservoir model is the key tool to understand and predict reservoir response to production load. The model should be consistent with estimated reservoir temperatures and pressures that govern the transfer of mass and heat in the system. It also ties together other conceptual models made by geological, geophysical, and geochemical studies. In this section, a conceptual model is presented for the Greater Zunil geothermal area.

It is important to note that the conceptual model presented is based on estimated reservoir temperatures and initial pressures from measured profiles, and some inaccuracies should be taken into consideration. Wells ZD-4 and 5 were estimated to be at BPD conditions, since their most recent profiles are not at equilibrium and were therefore not representative of the reservoir conditions (Appendix I). For the purpose of defining the boundaries of the reservoir, hypothetical wells were placed at the far edges of the study area. This does not influence the general distribution of temperature and pressure for Zunil I and II. The model is presented in two parts: (1) a close look at the Zunil I field; and (2) an overall model of Zunil I and II. Reservoir conditions for Zunil II are extrapolated from shallow drillholes and a clear picture of the deeper reservoir is not presented here.

6.1 Revised conceptual model of Zunil I

Reservoir temperature distributions in Zunil I show that a deep convecting liquid reservoir exists below 1100 m a.s.l. at temperatures near 300°C (see Figure 4). This reservoir is hosted in the granitic formation and may be fracture dominated. The fluids migrate upward and reach saturation conditions at the base of the volcanic formation. A second reservoir is present in the less permeable volcanic formation. The upper reservoir fluid is a mixture of deeper reservoir waters and downflowing recharge and condensed steam. The main feedzones in the upper reservoir are located at the contact between the granitic formation and the volcanic rocks and are characterized by poor permeability and flash into the formation.

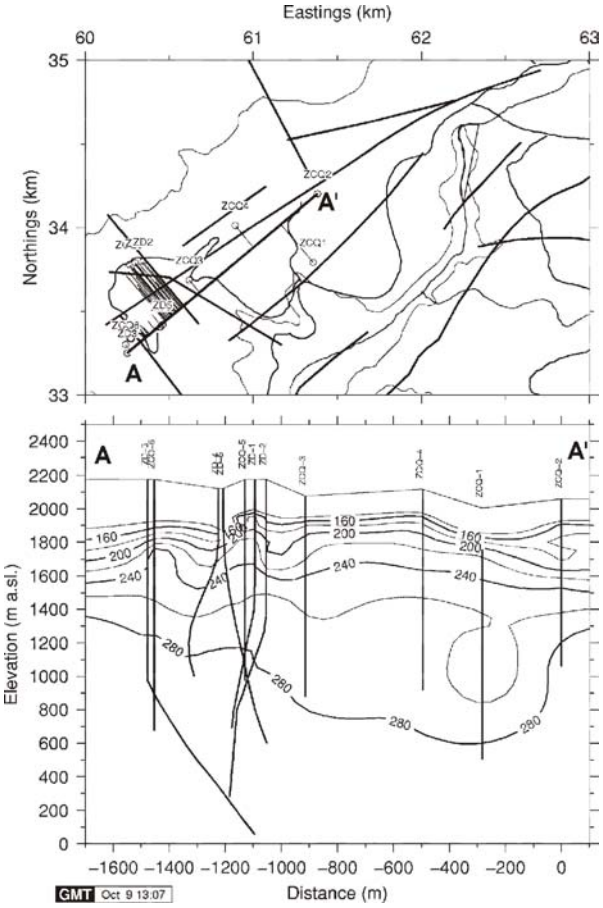

FIGURE 12: Reservoir temperature cross-section A-A' for Zunil I

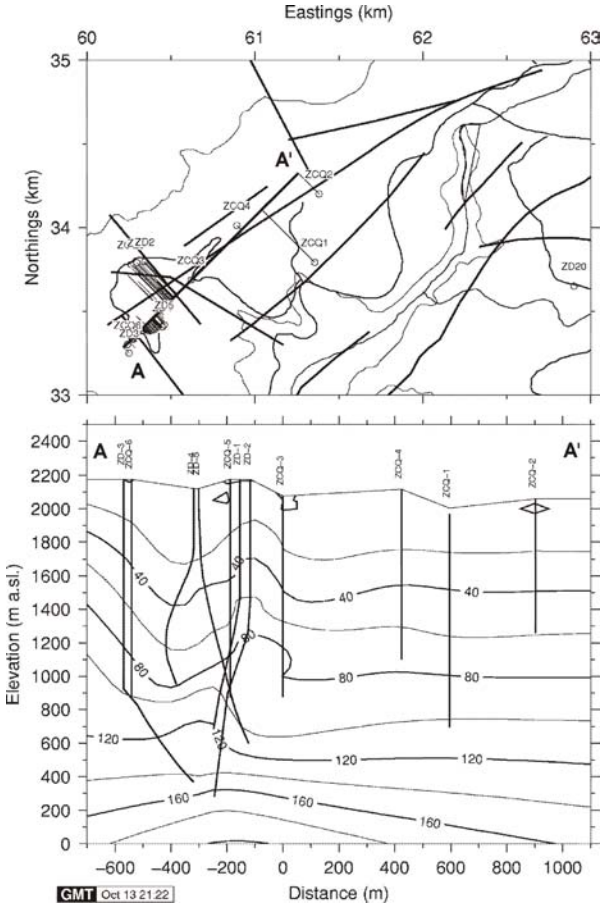

FIGURE 13: Reservoir pressure cross-section A-A' for Zunil I

Wells with feedzones in the shallow reservoir appear to have a poor connection to the surrounding reservoir, while wells that produce from fractures in the granitic formation have supposedly better pressure support from the reservoir.

Cross-sections along Zunil I for temperature and pressure are shown in Figures 12 and 13. Wells near the cross-sectional line have been projected. The temperature cross-section shows the main upflow is concentrated in the western area with an outflow near the central part of the field towards ZCQ-1 and 2 (Figure 12). Well ZCQ-2 appears to have high temperatures at depth and that may indicate a second upflow, possibly related to the fault along the Samala river to the west or to an intersection of faults just north of ZCQ-2. This may also suggest that the main upflow zone in the west is not circular, and could be a line source along a northeast trending fault. The pressure shows that the fluid is flowing up in the west along deep faults that extend into the granitic basement (Figure 13). The fluid flows to the west at a depth of 1100 m a.s.l. along the contact boundary between the granitic formation and overlying volcanics.

Temperature contours at 700 m a.s.l. are shown in Figure 14. The highest temperatures are located in the western part of Zunil I. This is consistent with the deeper convective reservoir and upflow zone. The upflow is near the intersection of two major fault trends that may act as conduits for the fluid to migrate upwards. Figure 15 shows temperature distributions at 1200 m a.s.l. near the permeable contact boundary between the granitic formation and volcanics. There is an outflow towards the northeast, and fluids are discharging in faults along Rio Samala. More data is needed below 1100 m a.s.l. for the eastern part of the study area to show whether the thermal anomaly is a separate upflow, or an extension of the main upflow.

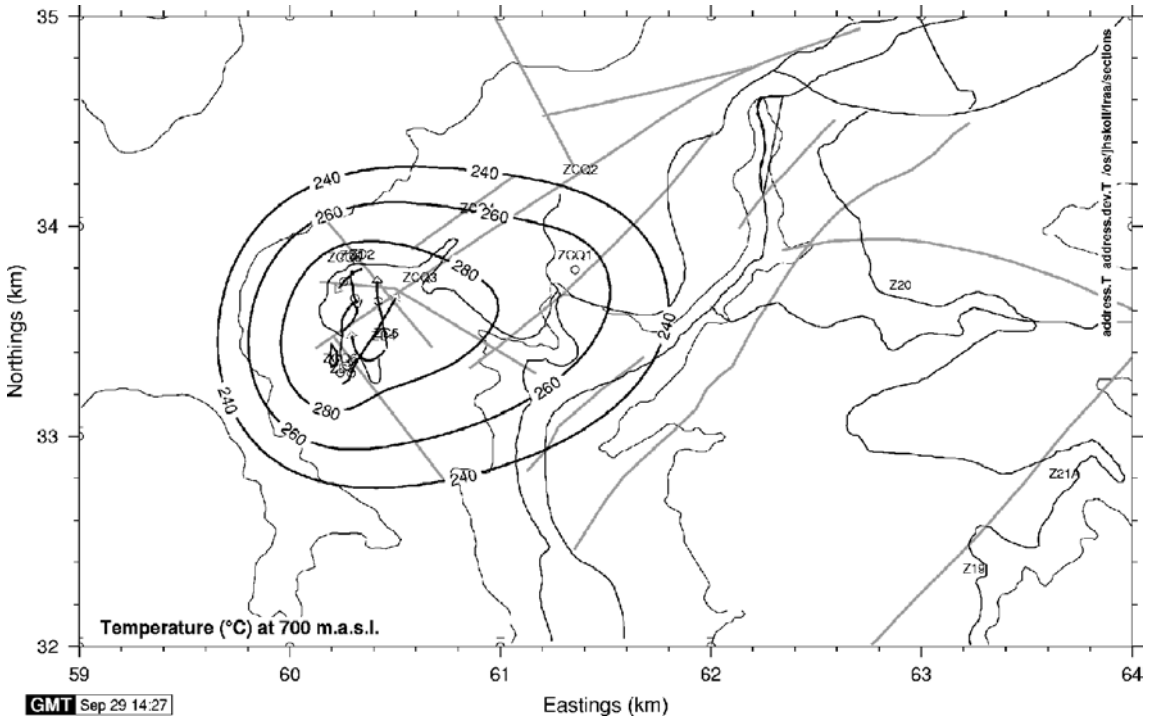

FIGURE 14: Temperature contours at 700 m a.s.l. for Zunil I

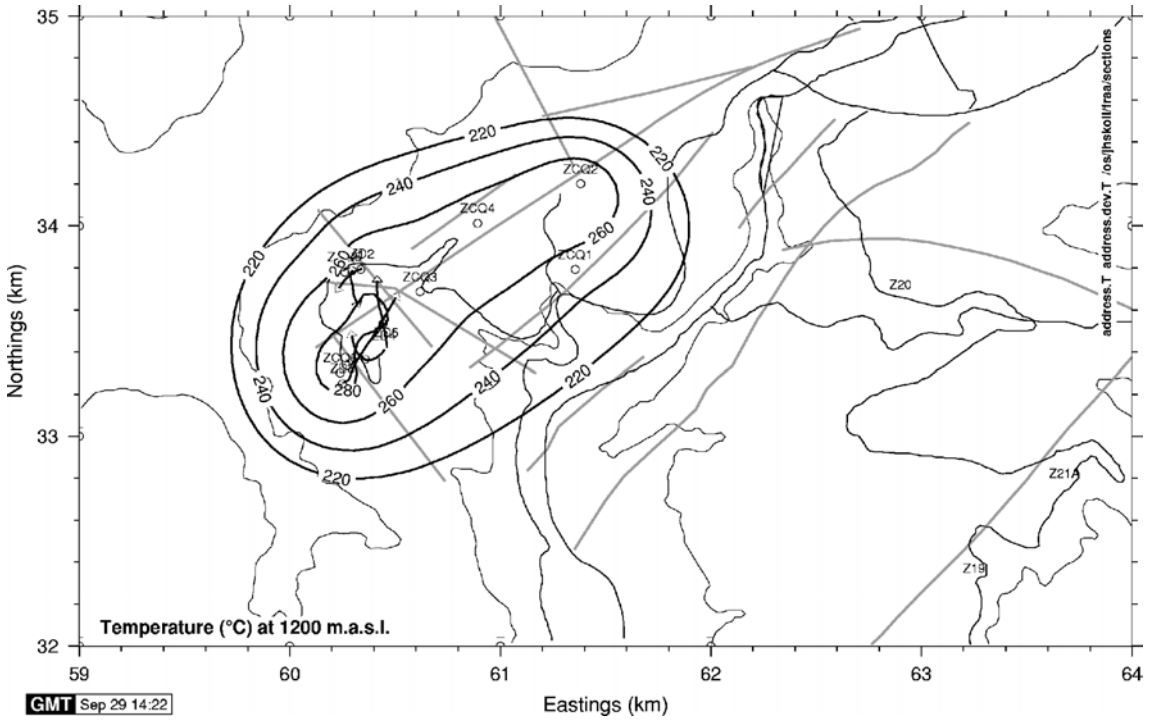

FIGURE 15: Temperature contours at 1200 m a.s.l. for Zunil I

The initial pressure distributions at 700 and 1200 m a.s.l. are shown in Figures 16 and 17, respectively. At 700 m a.s.l., the highest pressure potential is in the western area of the field with decreasing slope to the east (see Figure 16). At 1200 m a.s.l., the pressure distributions show the same pressure anomaly in the western area (see Figure 17). There appears to be a pressure sink near well ZCQ-5, close to higher

pressures recorded in ZD-1 and 2. This may be due to the fact that ZCQ-5 is connected to the less permeable upper reservoir with a lower pressure potential while ZD-1 and 2 have penetrated the deeper reservoir of higher pressure potentials. Inaccurate estimates of reservoir pressures for wells ZD-4 and 5 are seen as pressure lows (see Appendix I).

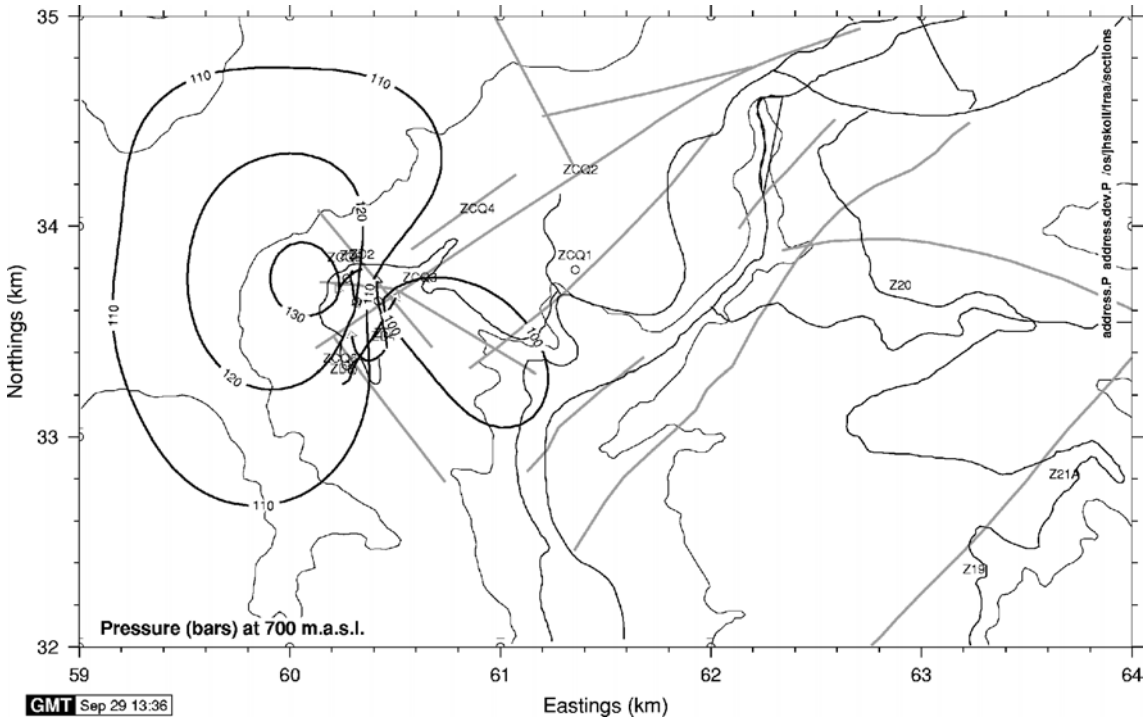

FIGURE 16: Pressure contours at 700 m a.s.l. for Zunil I

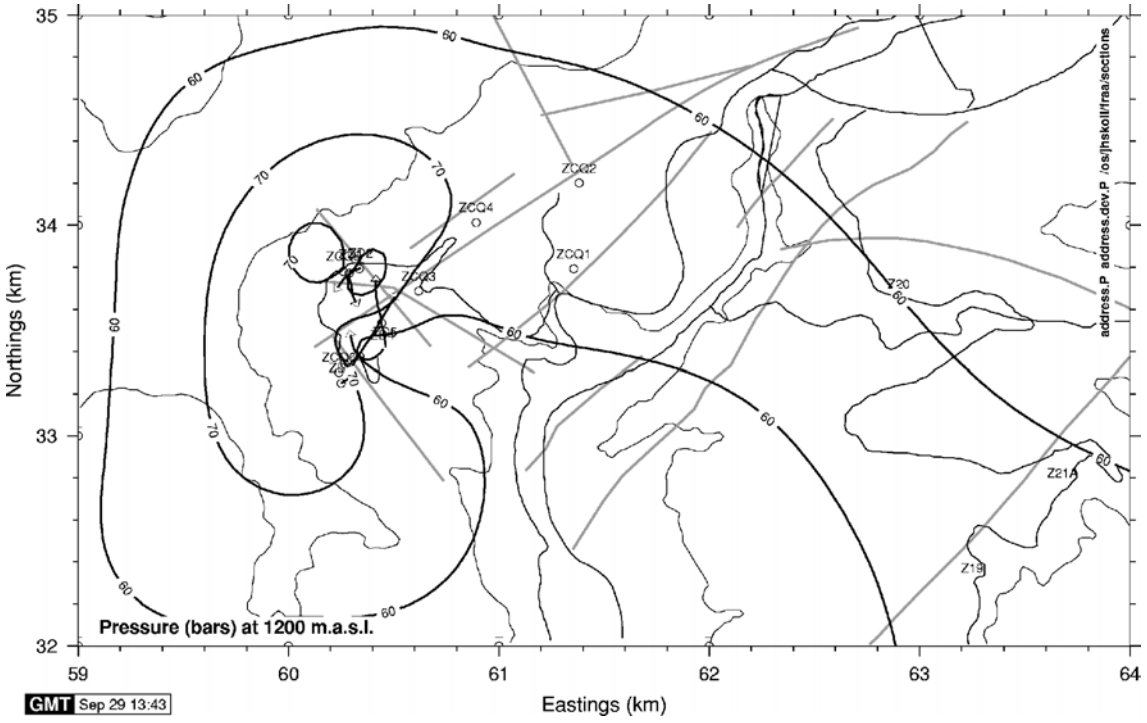

FIGURE 17: Pressure contours at 1200 m a.s.l. for Zunil I

6.2 A conceptual model of Zunil I and II

Reservoir temperatures and initial pressures presented in this study allow presentation of a conceptual model for the Zunil I and II geothermal fields. This model is shown in cross-section B-B[1] in Figure 18 and can be explained in the following terms:

a) The main upflow of fluids for Zunil I is located in the western part of the field at an intersection of two fault trends. A second heat source appears present near well ZCQ-2 (see Figure 12) and may be an extension of the main upflow.
b) A thermal anomaly is present near the south-eastern part of Zunil II (see Figure 19) and may indicate a possible upflow of fluids for Zunil II. Pressure potentials are higher in the southeast area with a downslope in the northwest direction (Figure 20). This may indicate that fluids are flowing out and discharging in faults near Rio Samala.
c) In Zunil I, a deeper, more permeable reservoir at liquid conditions lies within the granitic formation with temperatures not exceeding 300°C (see Figure 4).
d) The granitic contact with the overlying volcanics is present at 1100-1200 m a.s.l. for Zunil I and at 1800-1900 m a.s.l. for Zunil II. In Zunil I, this defines a permeable horizon. Wells with feedzones at this horizon have lower transmissivity and tend to flash in formation.

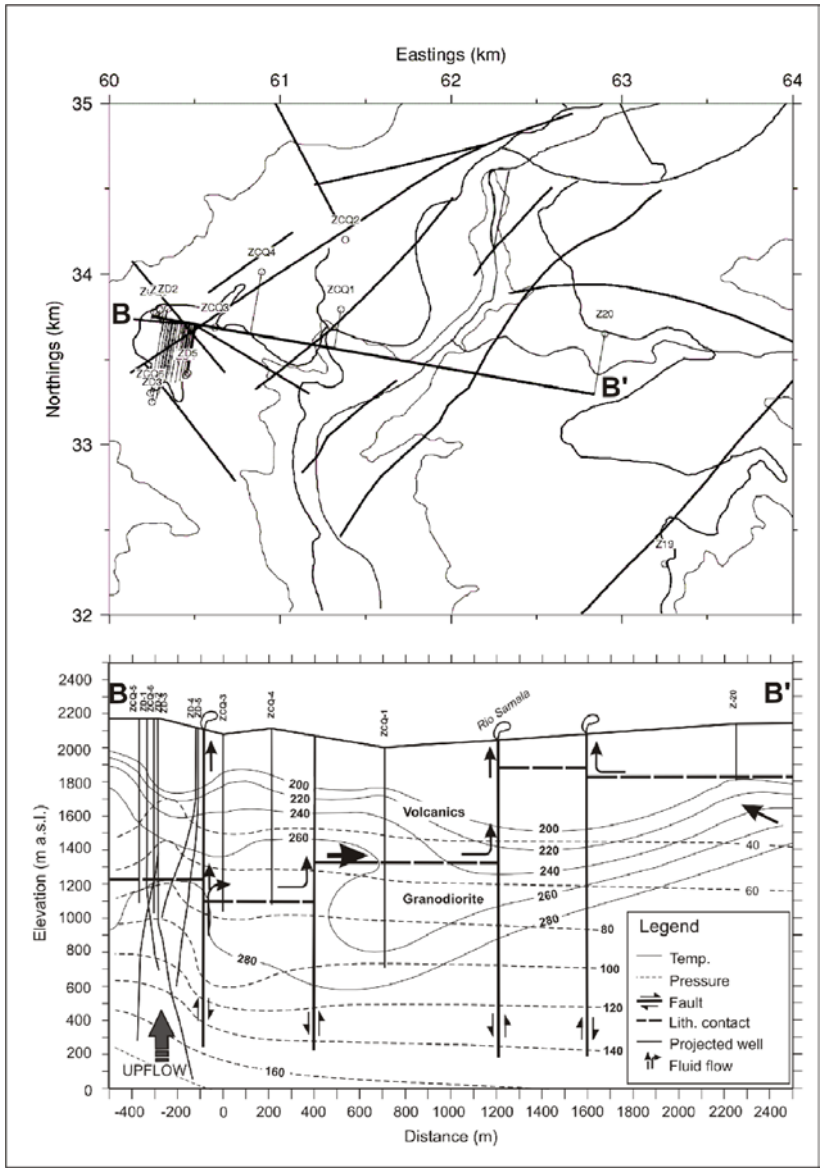

FIGURE 18: Conceptual model of Zunil I and II geothermal fields

e) Temperatures in Zunil II are much higher at shallow depths than towards the eastern side of Zunil I (see Figure 18). Extrapolated temperature profiles show that a reservoir may be present at shallower depth than Zunil I. Drilled shallow wells show temperature and pressures at saturation conditions. The reservoir may be hosted in the granitic formation and could be at liquid or close to saturation conditions.
f) A larger, E-W trending geothermal system is shown for Zunil I and II (Figure 19). The flow of fluids is possibly along permeable fractures associated with caldera margins of the Zunil Volcano for Zunil II. Pressure potential defines a similar E-W trending geothermal system (Figure 20). Fluids in the system are flowing to the northeast from Zunil I and to the northwest from Zunil II. The Zunil I and II systems seem to meet beneath the Samala river. This area appears to be the outflow of both systems.

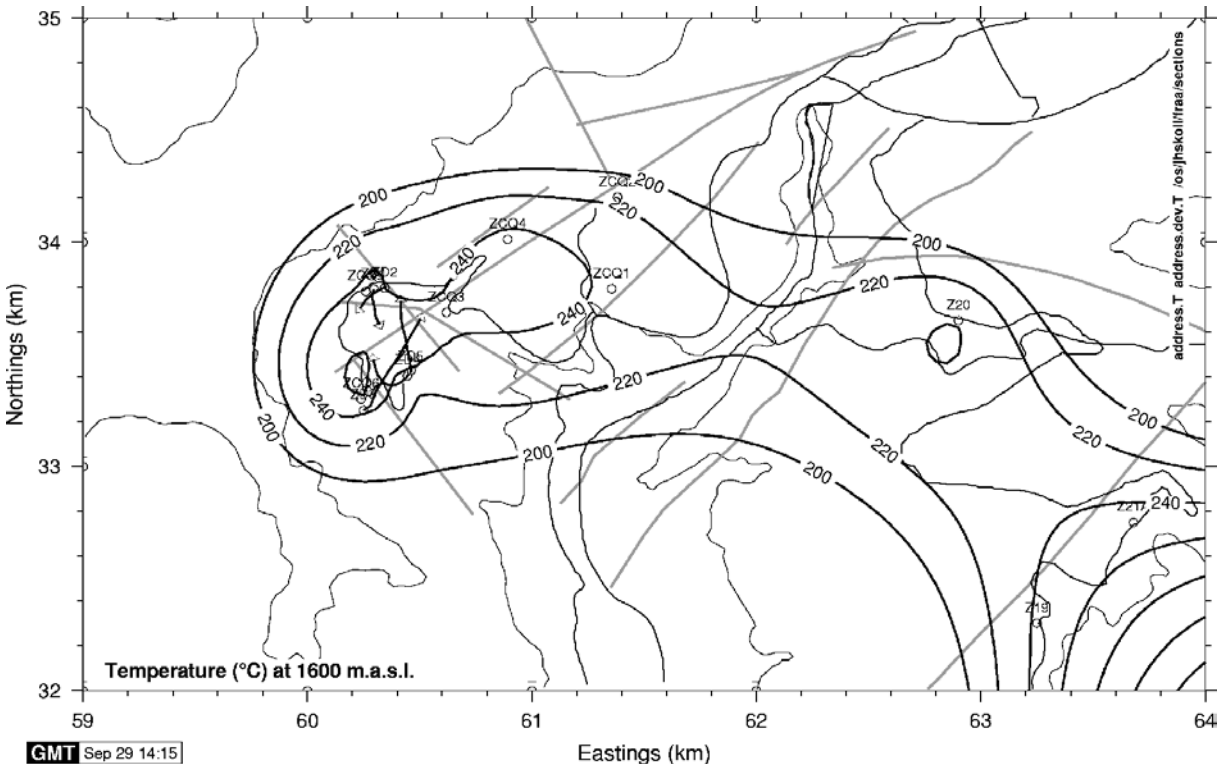

FIGURE 19: Temperature contours at 1600 m a.s.l. for Zunil I and II

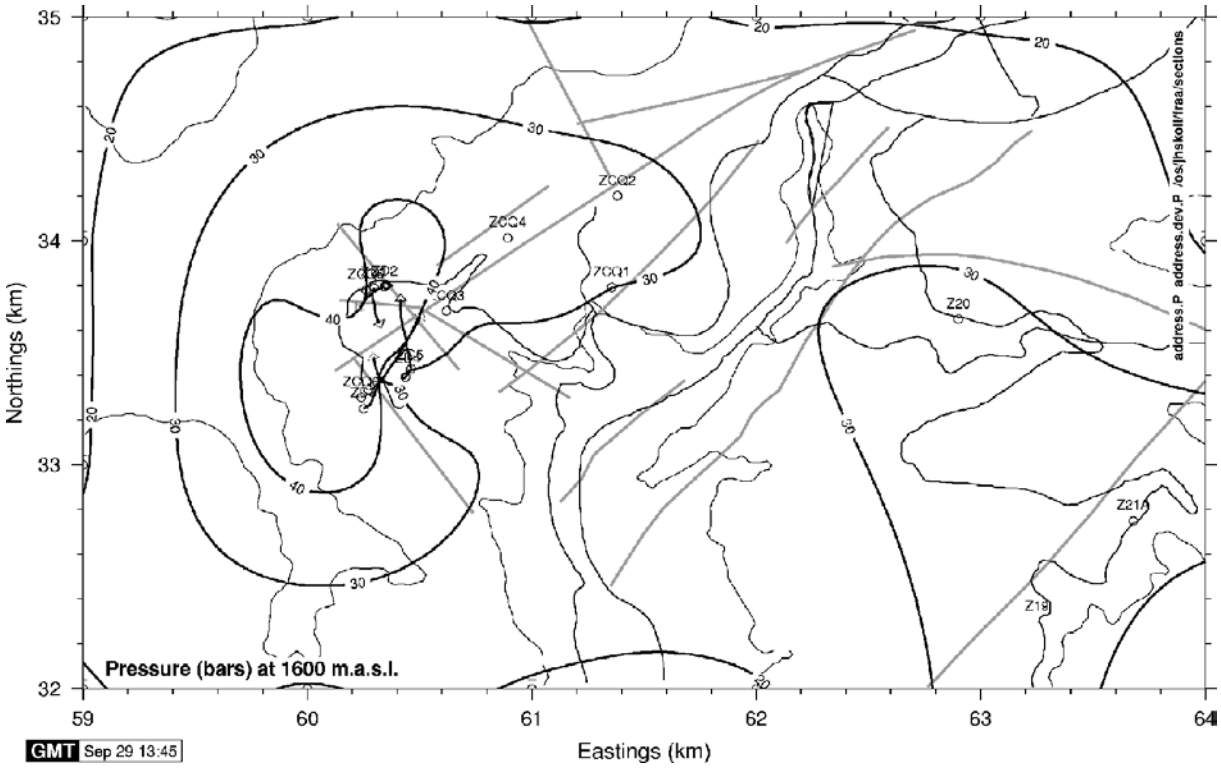

FIGURE 20: Pressure contours at 1600 m a.s.l. for Zunil I and II

7. VOLUMETRIC ASSESSMENT OF ZUNIL II

A volumetric estimate of the total amount of heat stored in a reservoir above some reject temperature is found very simply by volumetric interpretation of the temperature contours (Grant et al., 1982). This is a simple quantitative model for calculating the total "stored heat" in a reservoir when very little data is available for the reservoir. The following equations are used to calculate the power potential of a homogenous reservoir by estimating the amount of energy that can be extracted and converted to electricity:

$$E = V\rho_r C_r(1-\phi)(T-T_r) + V\rho_f\phi(h_f - h_r) \quad (5)$$

where E = Stored heat in the system (kJ);
V = Reservoir volume (m^3);
ρ_r, ρ_f = Density of rock and fluid (kg/m^3);
C_r = Heat capacity of rock (kJ/kg°C);
T, T_r = Initial reservoir temperature and final reference temperature (°C);
ϕ = Porosity of rock;
h_f, h_r = Initial fluid enthalpy in the reservoir and at final reference temperature (kJ/kg).

The equation that applies for converting the heat reserve into electrical power is given as:

$$Reserve\ (MWe) = \frac{E \times Recovery\ \ factor \times Conversion\ efficiency}{Plant\ life \times Load\ \ factor} \quad (6)$$

The uncertainty of reservoir parameters requires that they be estimated. For this reason, a Monte Carlo simulation is carried out. The simulation allows for the parameters to vary from a range of possible maximum to minimum values. The values within the range are calculated at random according to a triangular or square probability distribution function. The reserve is calculated several times from Equations 4 and 5, for each set of reservoir parameters. The results are plotted as a frequency distribution versus power output. Table 6 shows the estimated range of reservoir parameter values and the probability distribution function used to calculate them.

TABLE 6: Volumetric assessment parameters and their probability distribution for Zunil II

Property	Unit	Best guess	Probability distribution		
			Type	From	To
Area	km^2	3	Triangular	3	6
Reservoir thickness	m	1300	Triangular	700	1600
Rock density	kg/m^3	2300	Square	1670	2800
Rock porosity	%	9	Triangular	1	22
Water density	kg/m^3	783.9	Square	750.5	666.9
Reservoir temperature	°C	290	Square	280	320
Water enthalpy	kJ/kg	1134.5	Square	1236.8	1462.6
Rock heat capacity	kJ/kg°C	1.24	Constant	--	--
Reference temperature	°C	180	Constant	--	--
Reference water enthalpy	kJ/kg	763.1	Constant	--	--
Recovery factor	%	15	Square	10	15
Conversion efficiency	%	10	Constant	--	--
Load plant factor	%	85	Square	80	90
Plant life	Year	25	Constant	--	--

The distributed frequency and the potential electrical power for Zunil II are shown in Figure 21. The results of the simulation show that the Zunil II reservoir has potential between 25 and 45 MWe for 25 years. The cumulative frequency distribution indicates that the most likely value for the reserve is 35 MWe. The cumulative frequency graph also illustrates that there is less than a 10% chance that the reserve will be below 20 MWe. On the other hand, there is a 90% chance that the reserve will not yield 50 MWe. This means that if the field is planned for exploitation above 50 MWe, an additional reserve volume will need to be proven. It is important to point out that this simulation is based on volume estimates calculated by temperature distributions in Zunil II. The previous estimates for the field state that the total potential for Zunil II is 50 MWe. It is not clear what parameters were used in that study, but most likely they are based on a larger volume for the reservoir.

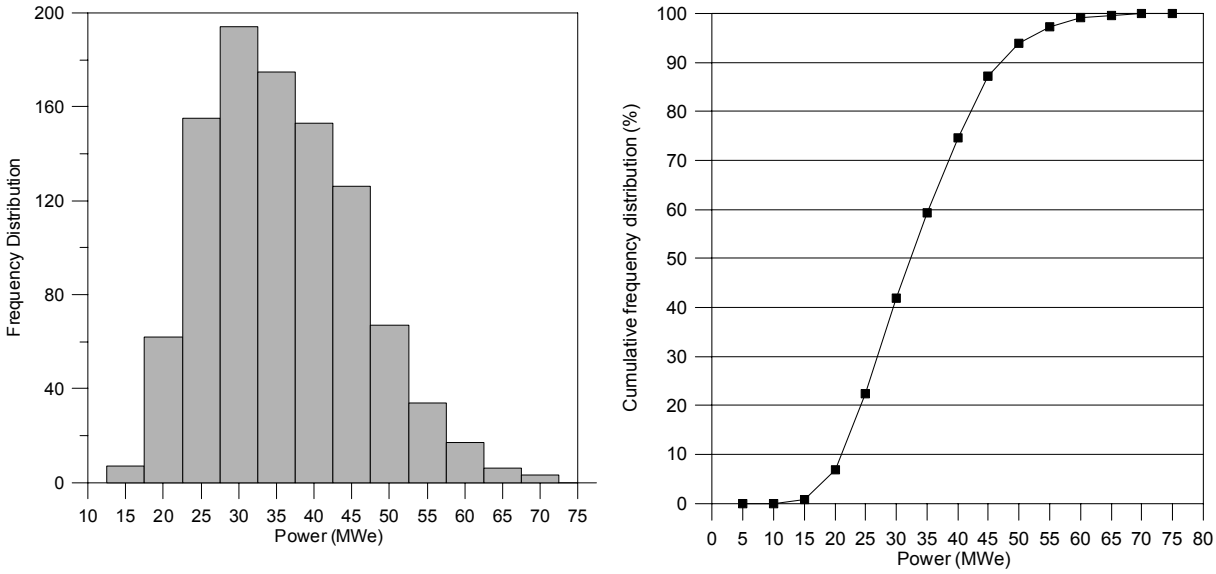

FIGURE 21: Frequency and cumulative frequency distributions for the reserve estimate of the Zunil II geothermal field

8. CONCLUSIONS AND RECOMMENDATIONS

8.1 Conclusions

The objective in this report is to present a reservoir assessment of the Zunil I and II geothermal fields from downhole temperatures and pressures. Based on the analysis of data available, the following conclusions and recommendations are put forward:

1. Downhole temperature and pressure for 14 wells were analysed. Reservoir temperatures and pressures were estimated and revised conceptual models for Zunil I and Zunil II were presented.

2. The Zunil I reservoir is divided into an upper and lower reservoir. The upper reservoir is lower in pressure, at 60-80 bar, while the lower reservoir has measured pressure at 80-120 bar.

3. Temperature and pressure contours at 700 and 1200 m a.s.l. show that there is an upflow in the western part of Zunil I. The upflow is consistent with an intersection of northeast and northwest trending faults. The outflow of hot fluids is to the northeast along faults trending in the same direction. A second thermal anomaly is present near ZCQ-2.

4. Overall permeability is low in the upper reservoir. The central part of Zunil I is hydraulically interconnected. The western part of the field and well ZCQ-2 do not show good connection with the central field.

5. Wells with producing feedzones in the upper reservoir produce at lithological contact boundaries. They tend to flash in the formation and yield less total flow than wells producing from the deeper, more permeable fractured granitic formation.

6. Wellbore simulations show that 100% re-injection in Zunil I will maintain reservoir pressures with minimal risk of temperature declines affecting total steam output.

7. Overall, higher temperatures are found at shallower depths in Zunil II than Zunil I, with a possible upflow in the southeast area and outflow towards the northwest at Rio Samala.

8. A larger, east-west trending, fracture-controlled geothermal system is defined for Zunil I and II. The size of the system is limited to the distribution of data available and may be much bigger.

9. Zunil II has a potential of 35 MWe for 25 years, based on Monte Carlo volumetric estimates.

8.2 Recommendations

1. Deeper wells are needed in Zunil II to define the reservoir size and characteristics.

2. Wells will have higher production rates if they are completed into the deeper reservoir in Zunil I.

3. A numerical simulation is needed for Zunil I and II to estimate the generating capacity of both fields.

4. Monitoring reservoir response to production needs to be improved for the Zunil area to assure the sustainability of the reserves.

ACKNOWLEDGEMENTS

I would like to give my sincerest gratitude to the United Nations University, the Government of Iceland, and to Dr. Ingvar B. Fridleifsson for giving me the opportunity to attend the UNU Geothermal Training Programme. I would also like to thank Lúdvík S. Georgsson for his tireless efforts and guidance throughout the course. I would like to thank my advisors Grímur Björnsson and Benedikt Steingrímsson for sharing with me all their knowledge and helping me to complete this study. To Mrs. Gudrún Bjarnadóttir for doing an excellent job of making sure that we felt at home in Iceland. To Maria-Victoria Gunnarsson for all her work in editing this report. To my new friends, the UNU-GTP 2003 Fellows, I thank all of you for your friendship and support.

I would like to thank Instituto Nacional de Electrificación for allowing me to come to Iceland for training. A special thanks to all my co-workers at Unidad de Desarrollo Geotérmico for providing me the information needed to complete this project.

I would like give a very special thanks to my family and friends who have been very supportive throughout my six months away from home.

REFERENCES

Adams, A., Goff, F., Trujillo, P.E., Counce, D., Medina, V., Archuleta, J., and Dennis, B., 1990: Hydrogeochemical investigations in support of well logging operations at the Zunil geothermal field, Guatemala. *Geothermal Resources Council, Transactions, 14-II,* 829-835.

Björnsson, G., Arason, P., and Bödvarsson, G.S., 1993: *The wellbore simulator HOLA. Version 3.1. User's guide*. Orkustofnun, Reykjavik, 36 pp.

Córdon y Mérida, MK Ferguson, and Morrison Knudsen Engineers Inc., 1990: *15 MWe geothermal-electric plant. Zunil I Quetzaltenango project: Integrated test program, final report.* Instituto Nacional de Electrificación – INDE, Guatemala, report (in Spanish).

Córdon y Mérida, MK Ferguson, and Morrison Knudsen Engineers Inc., 1991: *15 MWe geothermal-electric plant. Zunil I Quetzaltenango project: Geoscientific studies final report.* Instituto Nacional de Electrificación – INDE, Guatemala, report, 29 pp.

Córdon y Mérida, MK Ferguson, and Morrison Knudsen Engineers Inc., 1993: *15 MWe geothermal-electric plant. Zunil I Quetzaltenango project: Integrated test program, final report.* Instituto Nacional de Electrificación – INDE, Guatemala, report (in Spanish), 24 pp.

ELC-Electroconsult, 1980: *Zunil project, evaluation of field potential; igneous petrology and mineralogical alterations*. Instituto Nacional de Electrificación – INDE, report (in Spanish).

Foley, D., Moore, J.N., Lutz, S.J., Palma-A. J.C., Ross, H.P., Tobias-G, E., and Tripp, A.C., 1990: Geology and geophysics of the Zunil geothermal system, Guatemala. *Geothermal Resources Council, Transactions, 14-II,* 1405-1412.

Grant, M.A., Donaldson, I.G., and Bixley, P.F., 1982: *Geothermal reservoir engineering*. Academic Press Ltd., New York, 369 pp.

ISSCO S.A., 2000: *Evaluation of well ZCQ-4 and transmission pipeline. Zunil geothermal field, final report.* Instituto Nacional de Electrificación – INDE, Guatemala, report (in Spanish), 31 pp.

Lima, E.L., and Palma-A, J.C., 2000: The Zunil-II geothermal field, Guatemala, Central America. *Proceedings of the World Geothermal Congress 2000, Kyushu-Tohoku, Japan, 1,* 2133-2138.

Menzies, A.J., Granados, E.E., Sanyal, S.K., Mink, L.L., Merida, L., and Caicedo-A, A., 1990: An integrated test program for the definition of a high-temperature geothermal reservoir. *Geothermal Resources Council, Transactions, 14-II,* 1233-1239.

Moore, J.N., Lemieux, M.M., and Adams, M.C., 1990: The occurrence of CO_2 enriched fluids in active geothermal systems: Data from fluid inclusions. *Proceedings of the 15th Workshop on Geothermal Reservoir Engineering, Stanford University, California*, 193-198.

OLADE and BRGM, 1982: *Reconnaissance study of the geothermal resources of Guatemala, final report.* Instituto Nacional de Electrificación – INDE, Guatemala, report (in Spanish).

Palma-A, J.C., and Garcia, O., 1995: Update status of the development in Guatemala. *Proceedings of the World Geothermal Congress 1995, Florence, Italy, 1,* 135-140.

Palma-A, J.C., and Manzo, A.R., 2000: Guatemala geothermal energy development program for the next five years. *Proceedings of the World Geothermal Congress 2000, Kyushu-Tohoku, Japan, 1,* 407-412

Stefánsson, V., 1997: Geothermal reinjection experience. *Geothermics, 26*, 99-139.

Stefánsson, V., and Steingrímsson, B., 1990: *Geothermal logging I: an introduction to techniques and interpretation 3rd edition*. Orkustofnun, Reykjavik, report OS-80017/JHD-09, 117 pp.

Stoiber, R.E., and Carr, M.J., 1974: Quaternary volcanic and tectonic segmentation of Central America. *Bulletin of Volcanology, 37*, 304- 325.

West Japan Engineering Consultants Inc., Telectro S.A., and MK Ferguson Knudsen Engineers Inc., 1991: *Zunil II geothermal project. Pre-factibility study, selection of the most promising area.* Instituto Nacional de Electrificación – INDE, Guatemala, report.

West Japan Engineering Consultants Inc., Telectro S.A., and MK Ferguson Knudsen Engineers Inc., 1995: *Zunil II geothermal project. Pre-feasibility study*. Instituto Nacional de Electrificación – INDE, Guatemala, report (in Spanish), 45 pp.

Weyl, R., 1980: *Geology of Central America (*2nd completely revised edition). Gebruder Borntraeger, Berlin-Stuttgart, 371 pp.

APPENDIX I: TEMPERATURES AND PRESSURES FOR WELLS IN ZUNIL I AND II.

Zunil I wells

Well ZCQ-1: This well was the first production well to be drilled and is located in the central area of Zunil I. The maximum temperature recorded in this well is 270°C at the well bottom. The reservoir temperature profile is shown in Figure 1 and indicates heat conduction from surface and reaches boiling conditions at 225 m. The reservoir is boiling point with depth (BPD) down to 500 m. It falls back to single-phase liquid conditions and a reversal occurs from 700 down to 1000 m. The temperature rises at 1000 m down to the well bottom. Temperatures measured during warm-up show a feedzone just below the casing shoe, at a depth of 525 m and another one close to bottom depth. The well is primarily used as a re-injection well and has been sidetracked several times in order to increase the injection capacity. The reservoir pressure is hydrostatic down to the bottom of the well and shown in Figure 2.

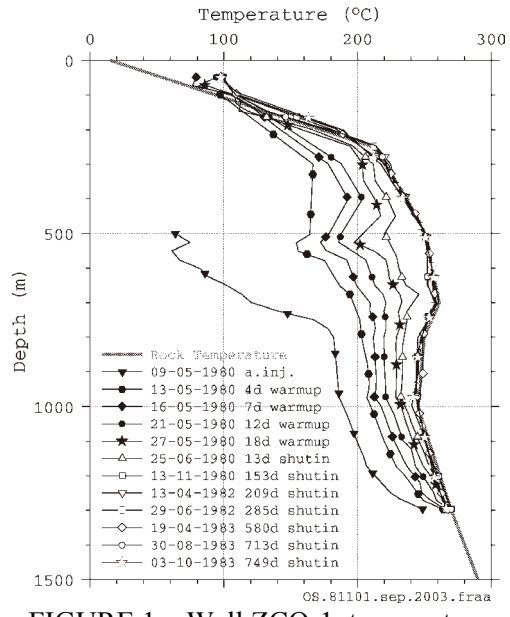

FIGURE 1: Well ZCQ-1, temperature logs and estimated formation temperature

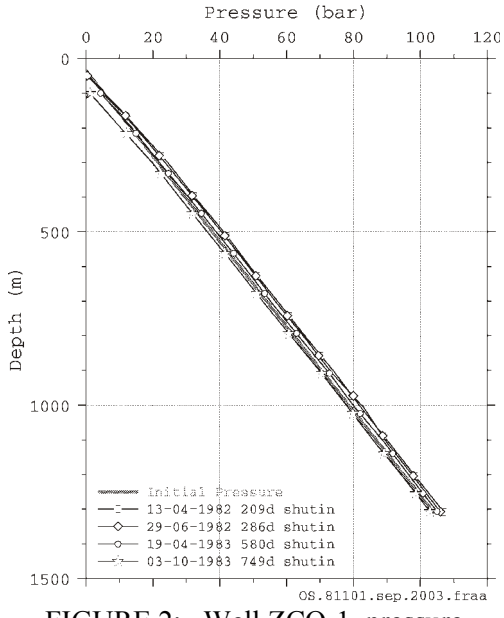

FIGURE 2: Well ZCQ-1, pressure logs and estimated initial pressure profile

Well ZCQ-2: This well is located in the northwest part of Zunil I and has a maximum recorded temperature of 268°C at 800 m. The reservoir temperature profile, shown in Figure 3, is conductive down to 75 m depth then follows BPD to 150 m. A temperature reversal is seen at 250 m indicating cooler aquifers behind the casing. The temperature rises at 500 m to BPD and a convective system is present down to the bottom of the well. Injection tests performed in 1989 gave an injectivity index of 1.2 l/s-bar using a flow of 14 kg/s and a water temperature of 50°C (Córdon y Mérida et al., 1991). Temperature logs show that the injected fluid flows into a feedzone at 800 m depth. This well is used for re-injection. Reservoir pressure is hydrostatic down to the bottom of the hole and is shown in Figure 4.

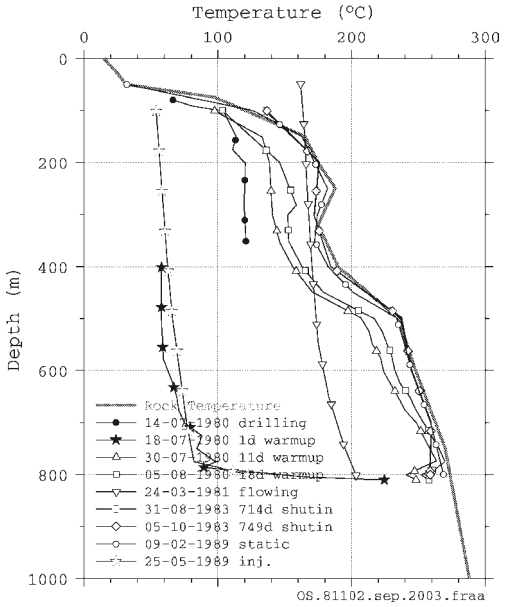

FIGURE 3: Well ZCQ-2, temperature logs and estimated formation temperature

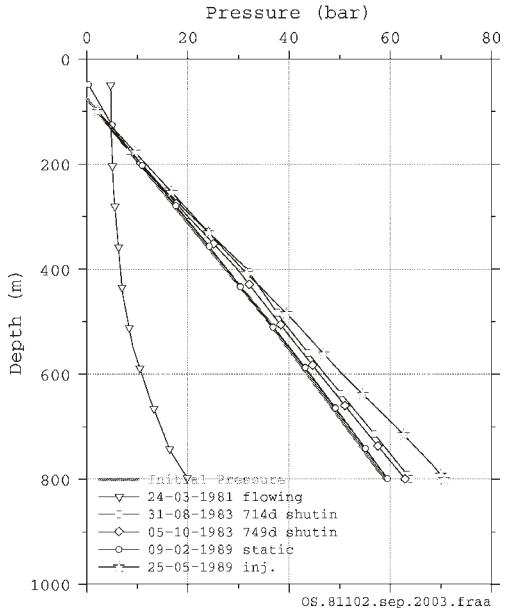

FIGURE 4: Well ZCQ-2, pressure logs and estimated initial pressure profile

Well ZCQ-3: The well is located in the central part of the field. It has a maximum recorded temperature of 268°C between 800 and 1000 m (Figure 5). The estimated reservoir temperature is BPD down to 750 m. The main feedzone is seen in measurements during the warm-up period (2 & 5-9-1980) as a sharp temperature increase from 650 to 700 m; some permeability is near well bottom.

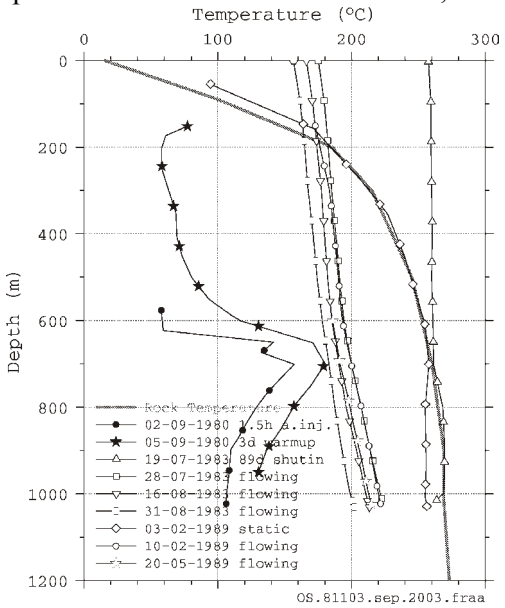

FIGURE 5: Well ZCQ-3, temperature logs and estimated formation temperature

On two separate flow tests, the enthalpy increased with time suggesting the fluid is flashing in the reservoir. A maximum enthalpy value of 1492 kJ/kg (Table 4 – main text) was calculated which is much higher than that indicated by dynamic profiles but is consistent with fluid flashing in formation picking up heat from the surrounding reservoir rock.

The pressure profile is shown in Figure 6 and follows measured logs taken on 22-07-1983. The reservoir pressure is hydrostatic down to the bottom of the well.

Well ZCQ-4: The well is located in the central section of Zunil I. The maximum temperatures for the well have been recorded at 270°C at the well bottom (Figure 7). Discharge tests showed that the well was cycling. Two separate feedzones were reported in previous reports, at 650-750 m and 800-850 m (Córdon y Mérida et al.,

1991; ISSCO, 2000). The main feedzone produces a high-enthalpy two- phase mixture and the second feedzone intermittently produces single-phase water. A shallower aquifer is identified from a temperature injection profile (30-01-1981) as a sharp kick in temperature just below the casing shoe at 480 m, but it is not clear if the two-phase feedzone is located here or at 650-750 m. The reservoir temperature is estimated to be conductive down to 130 m and increases along the BPD down to the bottom of the hole.

The reservoir pressure is estimated to be hydrostatic from 100 m down to the well bottom (Figure 8). Repeated pressure logs have measured different equilibrated pressures with time and could be explained by the cycling in the well as pressure shifts from feedzones. By decreasing the wellhead pressure, the cycling effects can be reduced.

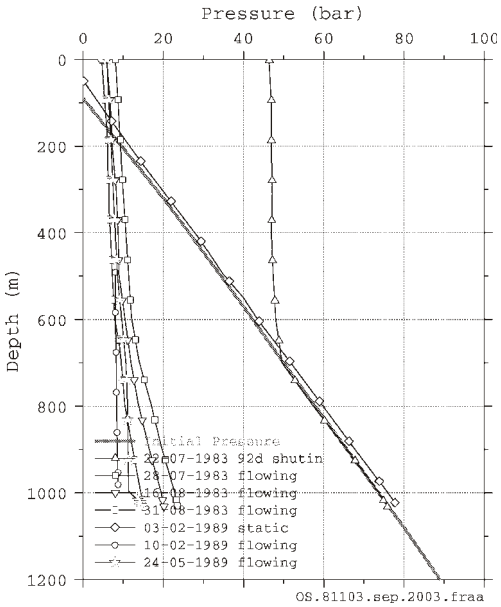

FIGURE 6: Well ZCQ-3, pressure logs and estimated initial pressure profile

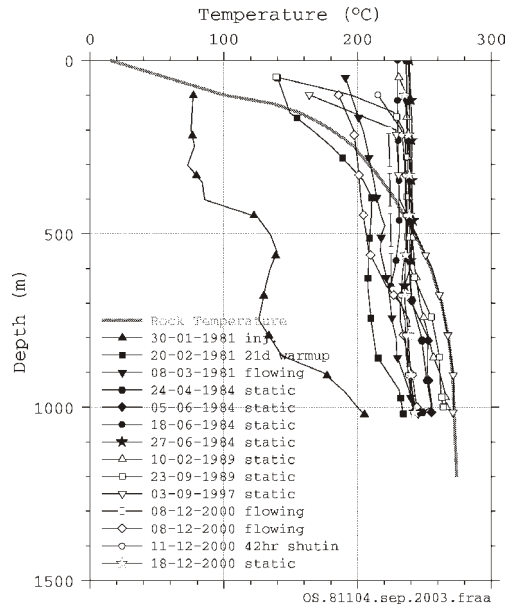

FIGURE 7: Well ZCQ-4, temperature logs and estimated formation temperature

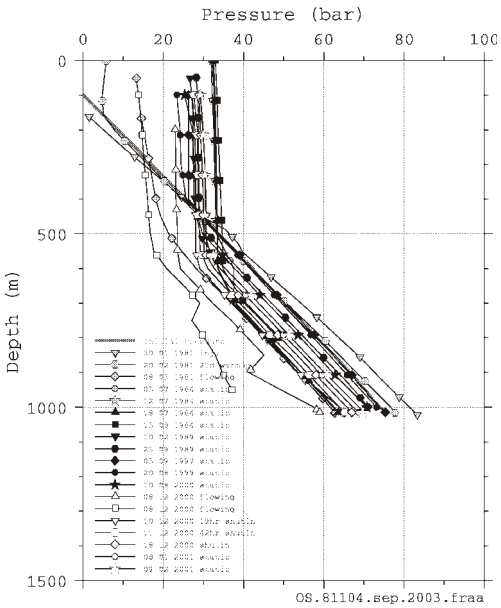

FIGURE 8: Well ZCQ-4, pressure logs and estimated initial pressure profile

Well ZCQ-5: This well is located near the central part of Zunil and resides close to the proposed upflow zone. Static temperature logs 30-01-1989 and 23-05-1989 are believed to be in equilibrium with the reservoir temperatures (Figure 9). The temperature increases by conduction down to 150 m and then along the BPD to 550 m. A convective system with fluid at single-phase liquid exists from 550 down to 950 m. The temperature increases back to BPD at 1050 m and it may be that a liquid reservoir exists at depth. It is believed that the ZD wells have penetrated down to this deeper reservoir.

During discharge tests, an erratic cyclic behaviour was observed (Córdon y Mérida et al., 1991). Although not as bad as well ZCQ-4, the well produced mainly a high-enthalpy two-phase mixture with sudden bursts of water represented by an increase in mass flow. A feedzone is consistent with the granitic basement contact and the overlying volcanic rocks at a depth of 950 m. Another aquifer is seen as an increase in temperature measured at 800 m 14 days after injection measured on 26-06-1981. The cycling could be explained by two separate feedzones, with different pressure potentials.

Pressure for well ZCQ-5 is estimated to be represented by static measurement recorded on 30-01-1989 (Figure 10). The initial pressure is hydrostatic from 150 m down to the well bottom.

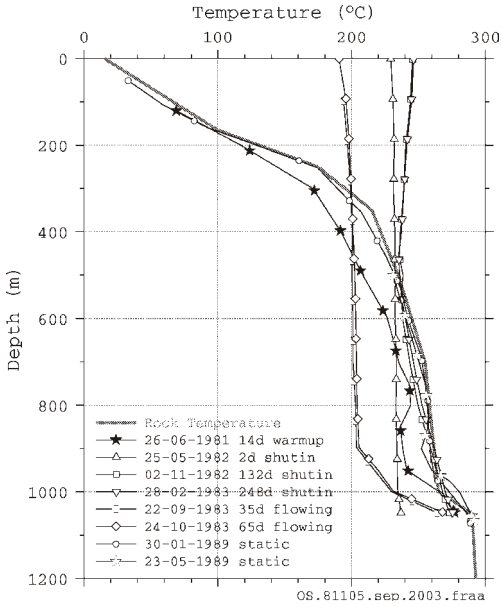

FIGURE 9: Well ZCQ-5, temperature logs and estimated formation temperature

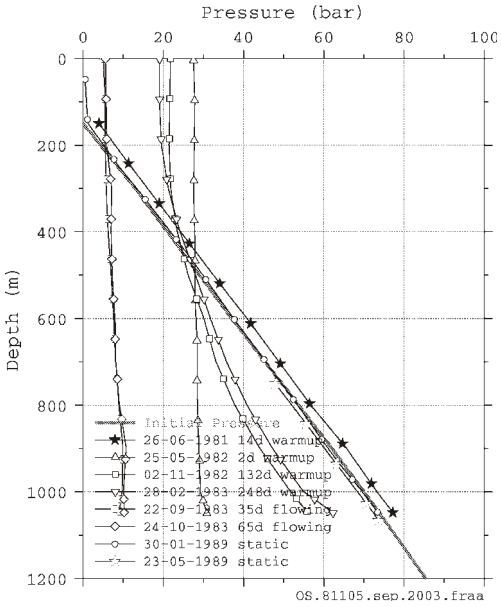

FIGURE 10: Well ZCQ-5, pressure logs and estimated initial pressure profile

Well ZCQ-6: This well is located over the proposed upflow zone in Zunil I. It has a maximum temperature of 289°C measured at a depth of 1000 m (Figure 11). Accumulation of steam and gas from boiling has disturbed some of the static logs. Reservoir temperature is estimated to closely resemble measured temperature for undisturbed conditions (11-12-1981). Conductive heating dominates temperatures above 400 m where it becomes convective down to well bottom along the BPD. The main aquifer is located at a depth of 1125 m identified by a total loss of circulation during drilling.

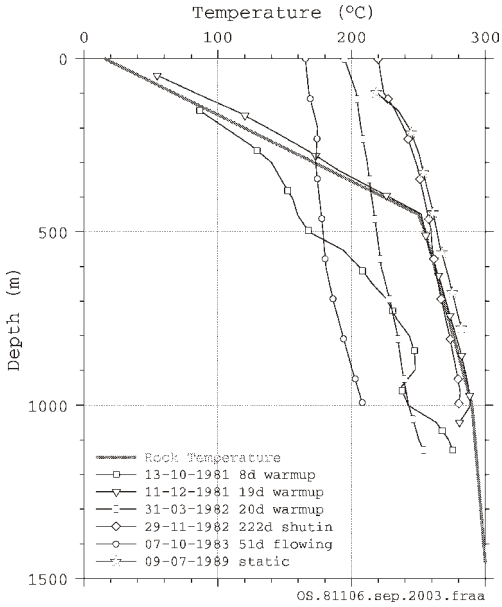

FIGURE 11: Well ZCQ-6, temperature logs and estimated formation temperature

Flow rate and enthalpy values stayed constant during discharge tests. The calculated enthalpy is higher than enthalpy values from flowing surveys, indicating that flashing is occurring in formation. The pressure profiles are affected by steam and gas build-up in the well. Figure 12 shows the estimated hydrostatic reservoir pressure.

Well ZD-1: The first well intended to penetrate the deeper Zunil I reservoir was ZD-1. The well is deviated and has a total measured depth of 1516 m and a total vertical depth of 1497 m. Figure 13 shows that the temperature in the reservoir is believed to follow the measured logs in the well (05-07-1991). The reservoir temperature increases from convective heating down to 600 m where the temperature reaches BPD. Temperatures increase from 700 m to a maximum temperature of 300°C measured at the well bottom. The reservoir temperature in this well is higher than in any of the ZCQ wells. The main feedzone is shown in the warm-up profiles at a depth of 1450 m. The well

produces from a fissure in the granitic rock where the deeper Zunil I reservoir resides.

This well is the best producer in Zunil I. During discharge tests, the enthalpy maintained fairly constant. It is presumed that the producing aquifer is at single-phase since measured enthalpy is fairly close to calculated enthalpy values from a dynamic temperature profile.

The pressure in the reservoir is at single-phase liquid conditions and hydrostatic for the most part (Figure 14). Measured pressure at the feedzone is 122 bar. The flashing point in the well is seen in the measured profile taken on 23-09-1992 at about 1000 m. Pressure in the reservoir is hydrostatic down to the bottom of the well.

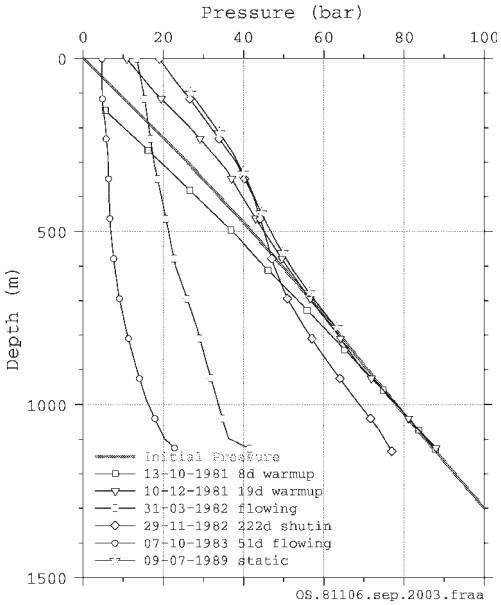

FIGURE 12: Well ZCQ-6, pressure logs and estimated initial pressure profile

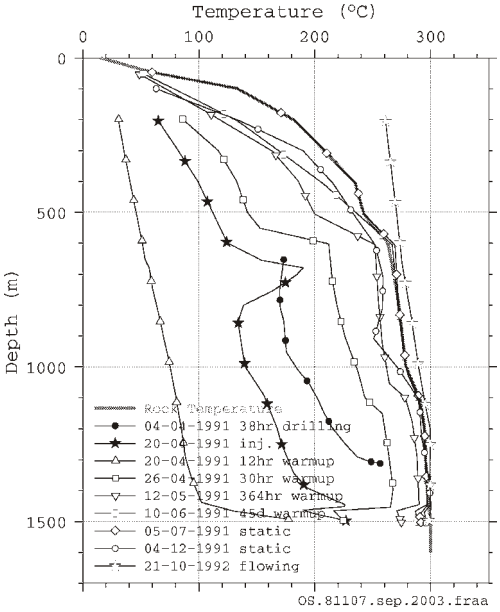

FIGURE 13: Well ZD-1, temperature logs and estimated formation temperature

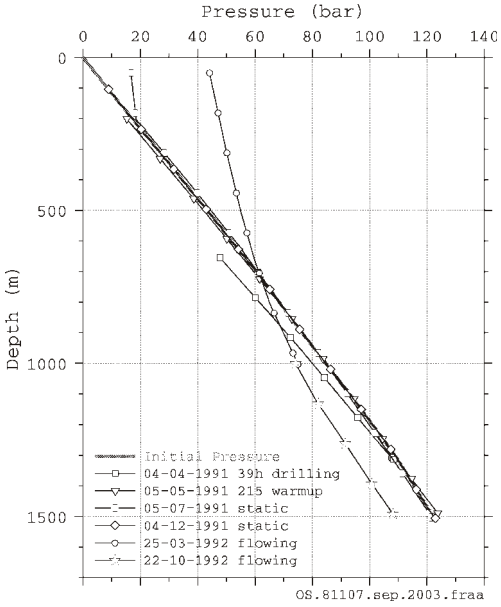

FIGURE 14: Well ZD-1, pressure logs and estimated initial pressure profile

Well ZD-2: This well is located in the western part of Zunil I. It was drilled down to a vertical depth of 1761 m and targeted into the deeper reservoir in Zunil I. The temperature profiles during drilling and warm-up show changes in temperature at 600, 900, 1300, 1440 and 1700 m suggesting aquifers at those depths (Figure 15). The main feedzone at 1460 m is found in the granitic basement rock and production is from the deeper reservoir. The reservoir temperature profile increases down to 300 m with a slight change in slope from 400 to 700 m as the reservoir becomes convectively heated. Convective heating is from 700 m down to the well bottom. The highest temperature of 298°C was measured at the well bottom where the reservoir is at liquid conditions.

Measured pressure at static condition (24-11-1991) is believed to be at equilibrium with initial pressures (Figure 16). The pressure of 120 bar is measured at the feedzone. A flowing profile shows flashing level in the well at 1000 m depth.

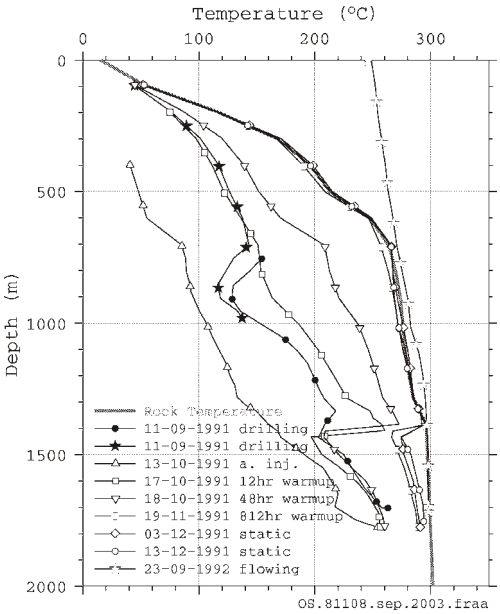

FIGURE 15: Well ZD-2, temperature logs and estimated formation temperature

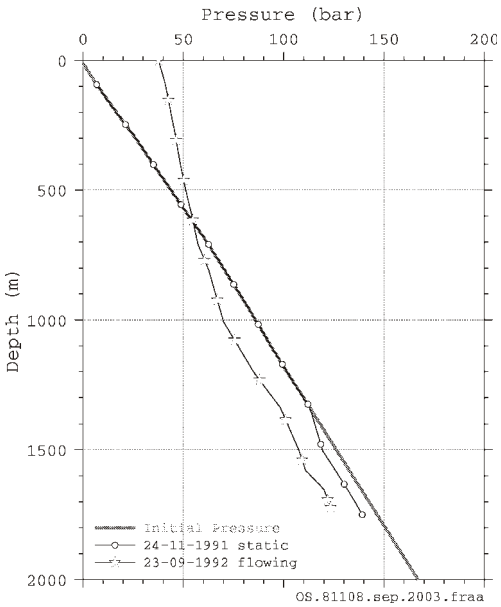

FIGURE 16: Well ZD-2, pressure logs and estimated initial pressure profile

Well ZD-3: This well is located in the western part of Zunil I. The well was drilled to a vertical depth of 2269 m and is the deepest well drilled in the Zunil area. Initially, the well had very low permeability but was successfully stimulated by injection. Measured temperatures during warm-up show kicks at 600 m, and from 1100 to 1200 m, indicating permeable horizons (Figure 17). The temperature in the reservoir is estimated to increase from conductive heating down to 300 m to BPD down to 1100 m. A slight temperature reversal is seen from 1100 to 1400 m, but it is not clear whether the reversal is due to internal downflow. A near constant temperature below the hot inflow suggests convection below 1100 m down to 1850 m. A second kick in temperature is recorded at the well bottom.

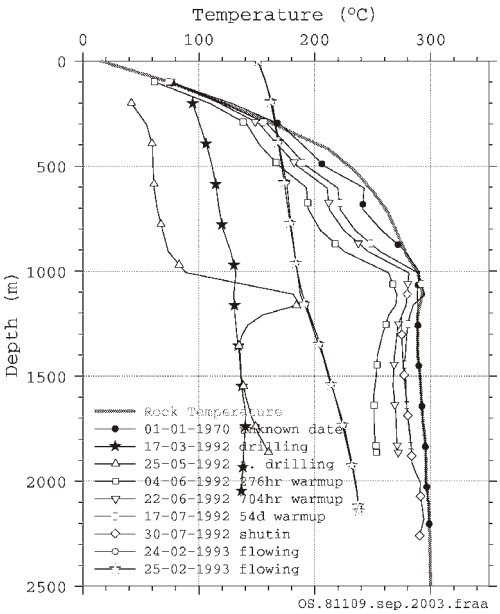

FIGURE 17: Well ZD-3, temperature logs and estimated formation temperature

Well tests showed that the wellhead pressure and the total flowrate decreased substantially during discharge. This may be the result of low permeability and/or well damage during drilling. Enthalpy increased during discharge which indicates flashing in formation. The flow characteristics of this well are more like the ZCQ wells than the two previous ZD wells (Table 4 – main text). The feedzone is located at the permeable contact between the volcanic rocks and the underlying granitic basement. The shallow producing wells all have permeable zones at this contact while ZD-1 and 2 produce fractures at greater depths.

Measured pressures on 11-06-1992 and 17-07-1992 show a pivot point at 1000 m that coincides with a feedzone seen in temperature measurements (Figure 18). It is not clear from the surveys if this is the main producing feedzone. The pressure in the reservoir appears to be hydrostatic from 20 m down to the well bottom with a pressure of 78 bar at the feedzone. The fluid next to the well is at single-phase liquid conditions below 1100 m.

Well ZD-4: This well is located near the centre of the field. It was drilled to a vertical depth of 1180 m. Temperature measurements during injection on 02-09-2001 show an aquifer at 1175 m (Figure 19). The reservoir temperature increases by conductive heating becomes saturated at 220 m down and follows then BPD to the well bottom. It is important to note that the last temperature log on 05-11-2001 was recorded when the well had not completely heated after drilling. The reservoir temperature was estimated to be BPD, consistent with other wells in the area.

Pressure measurements show effects of dense fluid that is not completely heated. The initial pressure was calculated using the program PREDYP (Figure 20).

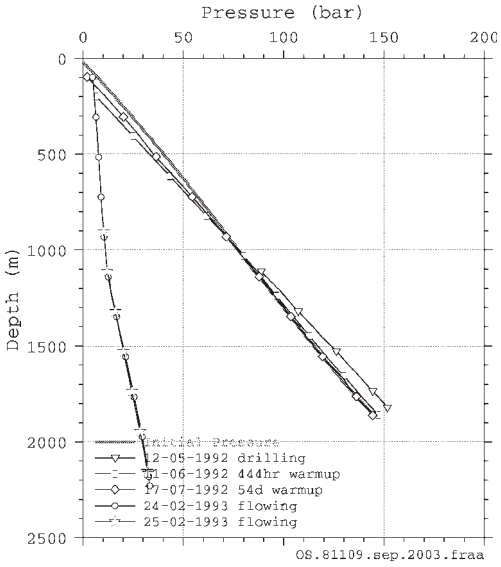

FIGURE 18: Well ZD-3, pressure logs and estimated initial pressure profile

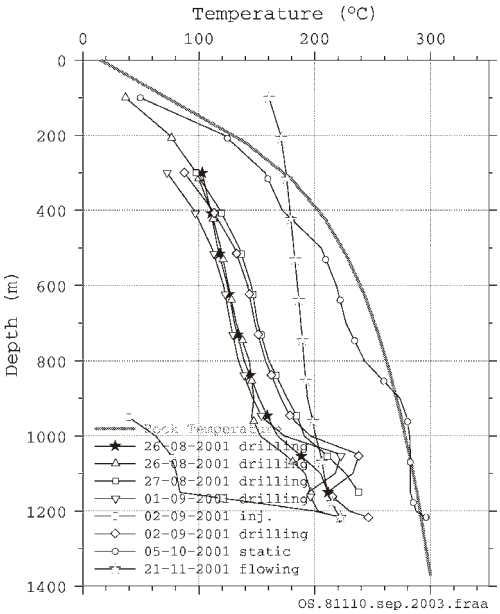

FIGURE 19: Well ZD-4, temperature logs and estimated formation temperature

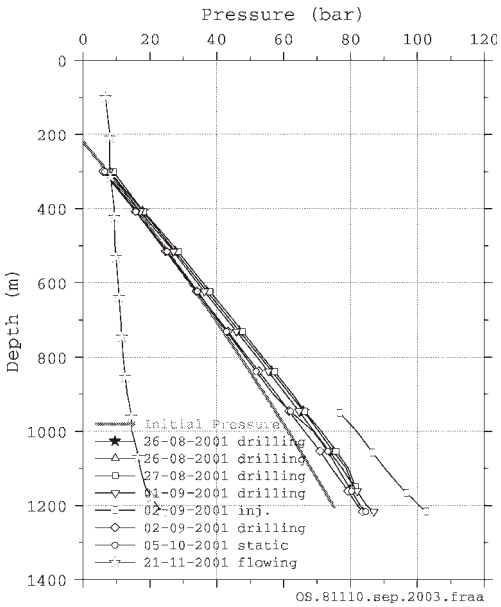

FIGURE 20: Well ZD-4, pressure logs and estimated initial pressure profile

Well ZD-5: The well is located in the centre of the field. It was drilled to a vertical depth of 1575 m. The well has very little permeability and repeated attempts to flow the well have been unsuccessful. The measured temperature logs during warm-up, shown in Figure 21, show a kick in temperature from 1025 m to 1200 m. The reservoir temperature is estimated to be BPD since the most recent measurement available on 13-06-2001 was recorded before the well was completely heated up after drilling.

Pressure in the reservoir was calculated using PREDYP and is hydrostatic from 120 m down to the well bottom (Figure 22). The fluid is at single-phase liquid conditions below 1150 m.

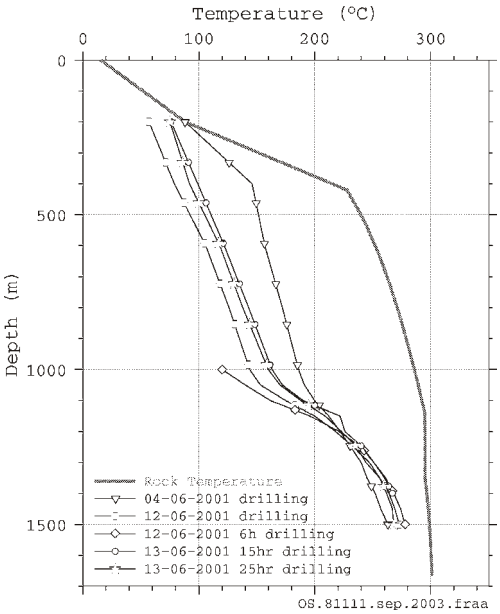

FIGURE 21: Well ZD-5, temperature logs and estimated formation temperature

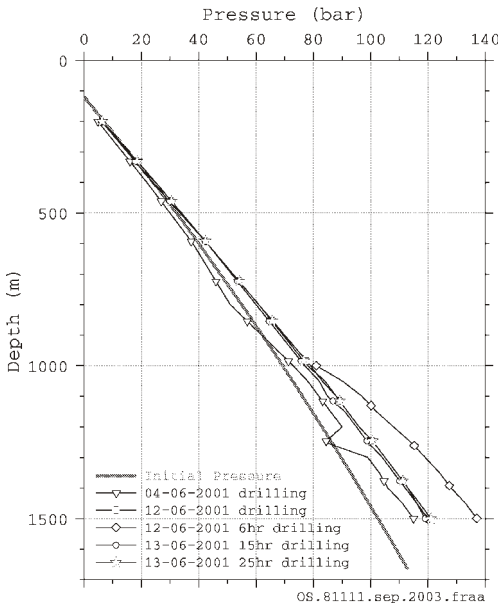

FIGURE 22: Well ZD-5, pressure logs and estimated initial pressure profile

Zunil II wells

Well Z-19: This 576 m deep well is located in the southern part of Zunil II. The estimated formation temperature is shown in Figure 23. The temperature increases by conductive heating down to 255 m and by BPD down to 400 m. The fluid is liquid water down to the bottom of the well. The logs are disturbed in the uppermost 300 m by steam and gas from the saturated fluid in the deeper section. The maximum downhole temperature of 204°C was recorded at well bottom. Pressure in the reservoir is estimated to be hydrostatic along the BPD from 255 to 400 m and single-phase pressure down to the bottom of the well (Figure 24).

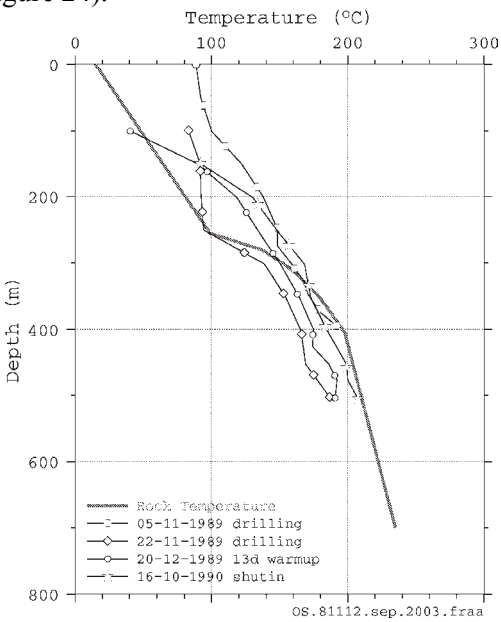

FIGURE 23: Well Z-19, temperature logs and estimated formation temperature

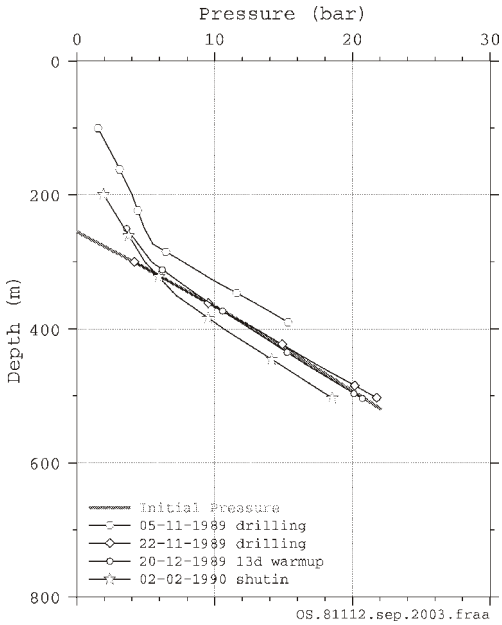

FIGURE 24: Well Z-19, pressure logs and estimated initial pressure profile

Well Z-20: The 364 m deep well is located in the southern part of Zunil II. The dowhole temperature conditions for this well were disturbed by steam and gas accumulated in the well. A maximum well

temperature of 207°C was measured at bottom (Figure 25). It is estimated that the formation temperature follows BPD from 165 m down to the well bottom, and that the fluid is at saturation (or oversaturated) at the well bottom. This would explain the accumulated steam inside the well. Pressure in the formation is assumed to be BPD from 165 m down to the well bottom (Figure 26). The highest measured pressure of 17 bar was down at the well bottom where the fluid is boiling.

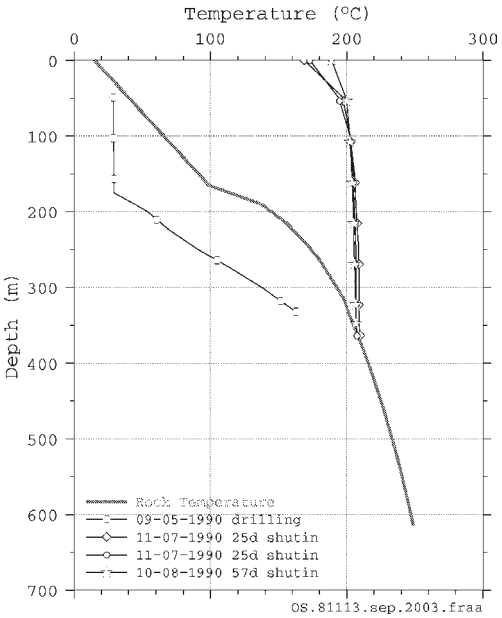

FIGURE 25: Well Z-20, temperature logs and estimated formation temperature

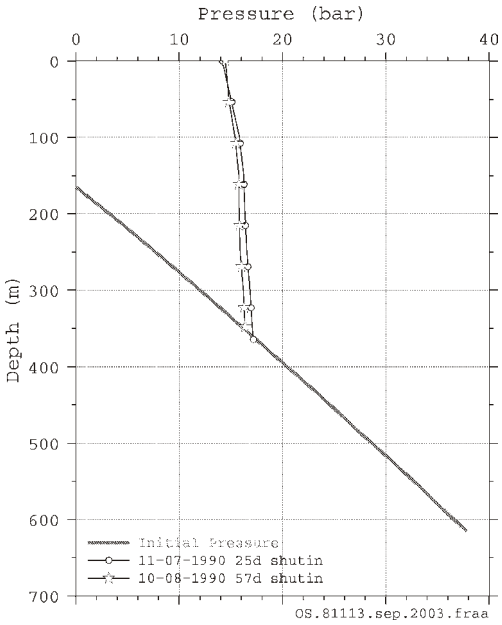

FIGURE 26: Well Z-20, pressure logs and estimated initial pressure profile

Well Z-21A: This 757 m deep well is located in the southern part of Zunil II. The reservoir temperature is slightly disturbed by steam and gas accumulation in the well. Figure 27 shows that temperature is conductive down to 295 m but increases, and then rapidly follows BPD to bottom. Attempts to make the well flow were done but were of limited success. The maximum temperature recorded was 244°C at the bottom of the well. The pressure profiles are affected by minor cycling within the well. The pressure of the reservoir is estimated to be hydrostatic along the BPD from 295 m down to the bottom (Figure 28).

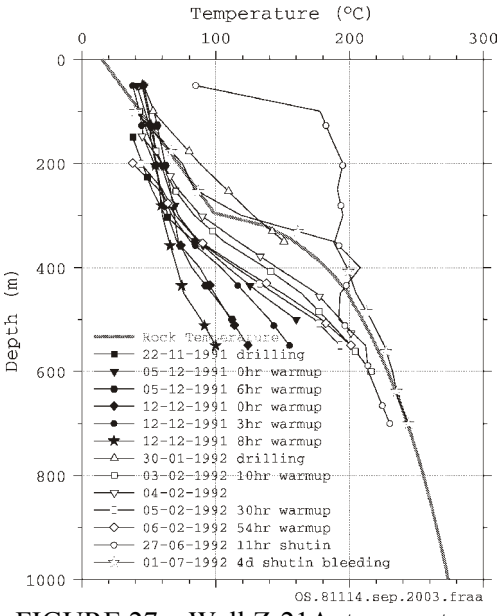

FIGURE 27: Well Z-21A, temperature logs and estimated formation temperature

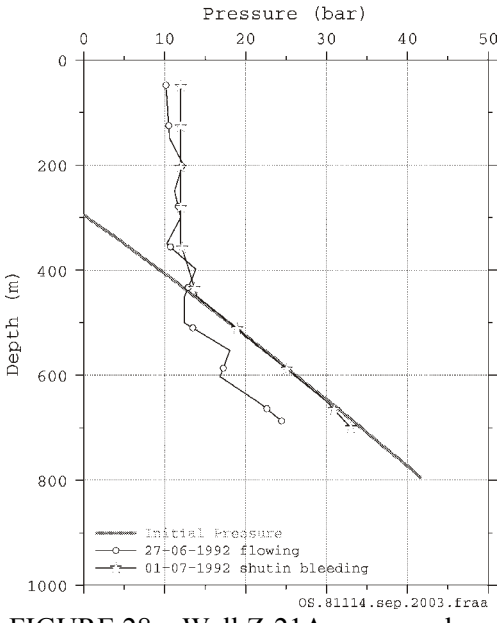

FIGURE 28: Well Z-21A, pressure logs and estimated initial pressure profile